Roles of GABAergic interneurons in calcium waves of the developing neocortex

Curtis R. Easton

A dissertation

submitted in partial fulfillment of the

requirements for the degree of

Doctor of Philosophy

University of Washington

2014

Reading Committee:

William J Moody, Chair
Robert F Hevner, Chair
Rachel O Wong
Martha M Bosma

Program Authorized to Offer Degree:
Neurobiology and Behavior

University of Washington

Abstract

Roles of GABAergic interneurons in calcium waves of the developing neocortex

Curtis R. Easton

Chair of the Supervisory Committee:

William J Moody
Biology

Robert F Hevner
Neurological Surgery
Pathology

Between early periods of brain development when genetic programs structure the basic features of the brain, and later periods when sensory-driven electrical activity refines neuronal connections, spontaneous activity generated by immature neurons plays a critical role in their development. In these studies we examine population activity in the developing neocortex: waves of action potentials propagating across the entirety of the cortex that may be measured with extracellular electrodes or optical techniques that measure cellular calcium influxes associated with waves. Using pharmacological and genetic blockade of neurotransmitter signaling we show complex roles for the neurotransmitter GABA in generating and regulating wave activity, as it may act almost simultaneously as an excitatory neurotransmitter in generating wave activity and also an inhibitory neurotransmitter that dampens the electrical oscillations of waves. Finally we use genetic expression of fluorescent proteins to label the GABA producing cells of the brain, inhibitory interneurons. We measure calcium activity in these cells and show that they express multiple types of calcium signals that may regulate different stages of cellular development.

Table of Contents

Page

General Introduction … *5*

Chapter One … *8*

Developmental changes in propagation patterns and transmitter dependence of waves of spontaneous activity in the mouse cerebral cortex.

Chapter Two … *22*

Genetic elimination of GABAergic neurotransmission reveals two distinct pacemakers for spontaneous waves of activity in the developing mouse cortex.

Chapter Three … *33*

Inhibitory interneurons exhibit both L-type calcium channel mediated, asynchronous calcium signals and TTX dependent population activity in developing Tbr1 deficient and wildtype neocortex

General Conclusions … *47*

General Introduction

There are many mechanisms by which the mammalian brain develops. Initially, signaling and guidance molecules help set the basic architecture of the brain. For example, sonic hedgehog (SHH) is a molecule that is distributed in a gradient with high levels in the ventral aspect of the forming neural tube and lower levels dorsally (Ericson et. al. 1995). Different levels of SHH lead to the differentiation of distinct cell types across the dorsal to ventral axis. A complex interaction of similar proteins across brain regions determines the morphology and connectivity of brain structures before the network is mature enough to support electrical activity. Then, later in development, electrical activity triggered by sensory input drives further brain development. Sensory deprivation during critical periods will lead to aberrant development of that particular sense; in the visual system, for example, depriving an animal of sight in one eye during a critical time in development will lead to permanent vision loss in that eye, whereas similar sensory deprivation applied later in life will have no permanent effects on vision (Hubel and Wiesel, 1963). But sensory driven electrical activity and signaling molecules are not the only factors driving brain maturation. A third mechanism influences brain development before sensory input matures: spontaneously generated electrical activity (Reviews: Moody and Bosma 2005, Hanganu-Opatz 2011). Maturing networks are prone to spontaneous depolarization on the cellular (Komuro and Rakic 1992, Bortone et. al. 2009) or population levels (Garashuk et. al. 2000, McCabe et. al. 2007, Meister et. al. 1991, Yang et. al. 2009) and these signals help to refine network architecture to enable sensory driven activity later on.

The specific type of spontaneous activity may differentially affect cell development. In addition to sodium mediated depolarization, developing cells experience spontaneous calcium influxes. Calcium oscillations have been shown to regulate proliferation of progenitor cells in the cortical ventricular zones (Weissman et. al., 2004), in addition to affecting the differentiation of progenitor cells into various cell types (Rosenberg and Spitzer, 2011 Review). And immature cells have been shown to use calcium channels to regulate cellular migration. But calcium oscillations in single cells are not the only form of spontaneous activity observed in developing brains. Once sufficient numbers of cells have been generated, immature networks experience network activity that involves action potential firing coordinated across neighboring cells in large brain regions. (Meister et. al. 1991, McCabe et. al. 2007) Neighboring cells are brought into the oscillations through synaptic contacts, gap junctions, or propagation of depolarization through the extracellular space (Moody and Bosma 2005, Hanganu-Opatz 2011). The evidence for roles of such activity in development is complex, and much research is focused on further elucidating these roles.

Parsing out the specific contributions to development of population activity can be a difficult task to accomplish. Single cell electrical depolarizations are occurring at the same developmental time as network oscillations in developing brains, and the two types of electrical activity may be dependent upon the same neural signaling mechanisms. For example, glutamatergic neurotransmission could trigger depolarization via non synaptic actions on individual, migrating neurons (Bortone et. al. 2009). However it is also necessary for coordinating and propagating population activity in the developing cortex (McCabe et. al. 2007). Thus, current theories on roles for population activity rely not so much on studies examining the effects of specifically blocking such activity in development, but rather by blocking all signaling through a particular neurotransmitter (Cang et. al. 2009), or considering the time and location of such activity with respect to the developmental processes occurring at that time. In the visual system, population activity in the retina is transmitted through the thalamus to the cortex (Ackman et. al. 2012). Such activity occurs just prior to eye opening, and studies have shown topographic map formation also begins just prior to eye opening (Hanganu-Opatz 2011) Thus a role for waves in establishing topographic maps has been proposed. Additionally, during the first postnatal week of

mouse development, inhibitory interneurons are integrating into the developing cortex just as population activity is occurring. Studies in cell culture have shown a potential role of population activity in signaling to these interneurons where they should reside in the cortex (de Lima et. al. 2009). This input of population activity on interneuron development could influence topographic map formation by using inhibition to sharpen boundaries of activation when a group of cells is depolarized by a stimulus in a specific part of the visual field.

The aim of this thesis is two-fold. One, to use genetic ablation of specific neurotransmitters and genetically encoded fluorescent indicator molecules to examine the contributions to population electrical activity of particular cell types. And two, to examine a putative role for population activity in the development of these cell types. We use the mouse neocortex as a model system, studying population activity measured with either extracellular electrical recordings, or calcium imaging techniques that allow visualization of calcium influxes in cells that occur during population activity. These studies build on past experiments that had shown population activity was expressed in coronal sections of mouse brain, initiated in ventral pacemaker regions and occasionally propagating into dorsal neocortex (Lischalk et. al. 2009).

Chapter One: Developmental changes in propagation patterns and transmitter dependence of waves of spontaneous activity in the mouse cerebral cortex.

In this study we examine two types of population activity observed in the developing neocortex: events which are restricted to the ventral cortex and run at high frequencies, and events which originate in the same brain regions but are able to propagate past the rhinal fissure and into the dorsal neocortex. We measure the frequencies of both types of activity over the course of their occurrence in development, hypothesizing that earlier activity in ventral regions is dependent upon excitatory neurotransmission from gamma-aminobutyric-acid (GABA), whereas later stage activity is dependent upon glutamatergic neurotransmission.

Chapter Two: Genetic elimination of GABAergic neurotransmission reveals two distinct pacemakers for spontaneous waves of activity in the developing mouse cortex.

To build upon the conclusions of the previous chapter, we utilize genetic manipulation of GABA synthesis to hypothesize the existence of two pacemakers for population activity in the developing cortex. We propose that early activity restricted to the ventral cortex is generated by an excitatory GABAergic pacemaker in the ventral cortex, while later in development, a glutamatergic pacemaker arises in the same location that generates population activity able to propagate into the dorsal neocortex. Additionally we construct a novel electrical recording device that allows us to simultaneously monitor brain activity with optical and electrical recording techniques, broadening the applications of the study by providing multimodal recordings that allow comparisons to more diverse studies. Finally we examine the interaction between the GABAergic and glutamatergic signaling networks and hypothesize a role for GABA not just in triggering population activity, but also in dampening glutamatergic network oscillations.

Chapter Three: Inhibitory interneurons exhibit both L-type calcium channel mediated, asynchronous calcium signals and TTX dependent population activity in developing Tbr1 deficient and wildtype neocortex

Here we hypothesize that genetic ablation of T-box, brain, 1 (Tbr1), a transcription factor responsible for patterning the developing cortex and proper differentiation of glutamatergic excitatory neurons there (Hevner et. al. 2001), will negatively affect the generation of population activity in the first postnatal week of mouse neocortex. We find that activity persists despite gross cortical malformations in the Tbr1 deficient animals, and identify two types of calcium signals in inhibitory interneurons in this mutant mouse which are labeled with red fluorescent protein: a signal restricted to single cells

and one which is synchronous across many cells in the field of view. We propose that these two signals are present in control and wild-type conditions and are distinct forms of activity that may regulate developmental functions such as the layer positioning of inhibitory interneurons, independent of molecular cues such as Tbr1. We hypothesize that the asynchronous signal is generated by L-type calcium channels (Bortone et. al. 2009) whereas the synchronous signal is selectively sensitive to blockade of sodium channels necessary for synaptically driven action potentials underlying population activity. The following studies will provide insight into the mechanisms generating population activity in the developing neocortex, and establish new techniques for examining the role of individual cell types in such activity. We focus on inhibitory interneurons, given the established roles of GABA in generating population activity in the cortex, but the methods used here are applicable to the study of any genetically distinct cell type. We hope these studies are useful not only for the information they provide about the role of inhibitory interneurons in calcium waves of the developing cortex, but also more broadly for those researchers looking to examine the specific contributions of particular cell types to other forms of brain activity.

References

Ackman JB, Burbridge TJ, Crair MC. (2012) Retinal waves coordinate patterned activity throughout the developing visual system. Nature. October 11; 490(7419): 219–225

Bortone D, Polleux F (2009) KCC2 expression promotes the termination of cortical interneuron migration in a voltage-sensitive calcium-dependent manner. Neuron. 62(1):53-71.

Cang J, Rentería RC, Kaneko M, Liu X, Copenhagen DR, Stryker MP. (2005) Development of precise maps in visual cortex requires patterned spontaneous activity in the retina. Neuron. Dec 8;48(5):797-809.

de Lima AD, Gieseler A, Voigt T (2009) Relationship between GABAergic interneurons migration and early neocortical network activity. Dev Neurobiol. 69(2-3):105-23.

Ericson J, Muhr J, Placzek M, Lints T, Jessell TM, Edlund T. (1995) Sonic hedgehog induces the differentiation of ventral forebrain neurons: a common signal for ventral patterning within the neural tube. Cell. Jun 2;81(5):747-56.

Garaschuk O, Linn J, Eilers J, Konnerth A. (2000) Large-scale oscillatory calcium waves in the immature cortex. Nat Neurosci. May;3(5):452-9.

Hanganu-Opatz IL. (2010) Between molecules and experience: role of early patterns of coordinated activity for the development of cortical maps and sensory abilities. Brain Res Rev. Sep;64(1):160-76.

Hevner RF, Shi L, Justice N, Hsueh Y, Sheng M, Smiga S, Bulfone A, Goffinet AM, Campagnoni AT, Rubenstein JL (2001) Tbr1 regulates differentiation of the preplate and layer 6. Neuron. 29(2):353-66.

Komuro H, Rakic P. (1992) Selective role of N-type calcium channels in neuronal migration. Science. Aug 7;257(5071):806-9.

Lischalk JW, Easton CR, Moody WJ. (2009) Bilaterally propagating waves of spontaneous activity arising from discrete pacemakers in the neonatal mouse cerebral cortex. Dev. Neurobiol. 69:407-14.

McCabe AK, Easton CR, Lischalk J, Moody, WJ (2007) Roles of glutamate and GABA receptors in setting the developmental timing of spontaneous synchronized activity in the developing mouse cortex. Dev. Neurobiol. 67:1574-1588.

Meister M, Wong RO, Baylor DA, Shatz CJ. (1991) Synchronous bursts of action potentials in ganglion cells of the developing mammalian retina. Science. May 17;252(5008):939-43.

Moody WJ, Bosma MM. (2005) Ion channel development, spontaneous activity, and activity-dependent development in nerve and muscle cells. Physiol Rev. Jul;85(3):883-941. Review

Rosenberg SS, Spitzer NC. (2011) Calcium signaling in neuronal development. Cold Spring Harb Perspect Biol. Oct 1;3(10):a004259. Review

Weissman TA, Riquelme PA, Ivic L, Flint AC, Kriegstein AR. (2004) Calcium waves propagate through radial glial cells and modulate proliferation in the developing neocortex. Neuron. Sep 2;43(5):647-61.

Wiesel, T.N. and Hubel, D.H. (1963) Single cell responses in striate cortex of kittens deprived of vision in one eye. J. Neurophysiol., 26: 1003-1017.

Yang JW, Hanganu-Opatz IL, Sun JJ, Luhmann HJ. (2009) Three patterns of oscillatory activity differentially synchronize developing neocortical networks in vivo. J Neurosci. Jul 15;29(28):9011-25.

Chapter One

Developmental changes in propagation patterns and transmitter dependence of waves of spontaneous activity in the mouse cerebral cortex.

Conhaim J, Easton CR, Becker MI, Barahimi M, Cedarbaum ER, Moore JG, Mather LF, Dabagh S, Minter DJ, Moen SP, Moody WJ.

(2011)

Journal of Physiology
May 15;589(Pt 10):2529-41.

J Physiol 589.10 (2011) pp 2529–2541

Developmental changes in propagation patterns and transmitter dependence of waves of spontaneous activity in the mouse cerebral cortex

Jay Conhaim, Curtis R. Easton, Matthew I. Becker, Mitra Barahimi, Emily R. Cedarbaum, Jennifer G. Moore, Luke F. Mather, Sarah Dabagh, Daniel J. Minter, Samantha P. Moen and William J. Moody

Department of Biology, University of Washington, Seattle, WA 98195, USA

Non-technical summary It is not well understood how all of the connections among neurons required for the brain to process information are established during development. It has recently become apparent that waves of spontaneous electrical activity spread across large groups of neurons during early brain development and that these waves of activity are crucial for correct development of brain circuitry. In this paper, we show that waves of spontaneous electrical activity propagate across the mouse cerebral cortex, beginning on the day before birth and continuing through the first 12 postnatal days. These waves are initiated at specific locations in the cortex, which do not change during the period of wave generation. Identity of the neurons that initiate the waves, however, does change during this time. This work indicates that even though spontaneous electrical activity occurs during a short contiguous period of development, the mechanisms underlying that activity change.

Abstract Waves of spontaneous electrical activity propagate across many regions of the central nervous system during specific stages of early development. The patterns of wave propagation are critical in the activation of many activity-dependent developmental programs. It is not known how the mechanisms that initiate and propagate spontaneous waves operate during periods in which major changes in neuronal structure and function are taking place. We have recently reported that spontaneous waves of activity propagate across the neonatal mouse cerebral cortex and that these waves are initiated at pacemaker sites in the septal nucleus and ventral cortex. Here we show that spontaneous waves occur between embryonic day 18 (E18) and postnatal day 12 (P12), and that during that period they undergo major changes in transmitter dependence and propagation patterns. At early stages, spontaneous waves are largely GABA dependent and are mostly confined to the septum and ventral cortex. As development proceeds, wave initiation depends increasingly on AMPA-type glutamate receptors, and an ever increasing fraction of waves propagate into the dorsal cortex. The initiation sites and restricted propagation of waves at early stages are highly correlated with the position of GABAergic neurons in the cortex. The later switch to a glutamate-based mechanism allows propagation of waves into the dorsal cortex, and appears to be a compensatory mechanism that ensures continued wave generation even as GABA transmission becomes inhibitory.

(Received 10 November 2010; accepted after revision 23 March 2011; first published online 28 March 2011)
Corresponding author W. J. Moody: Department of Biology, Box 351800, University of Washington, Seattle, WA 98195, USA. Email: profbill@u.washington.edu

Abbreviations E, embryonic day; P, postnatal day; PFA, paraformaldehyde.

Introduction

Spontaneous electrical activity plays widespread and important roles in the development of nervous systems, in both vertebrates and invertebrates (see Moody & Bosma, 2005 and Blankenship & Feller, 2010, for reviews). In the mammalian CNS, spontaneous activity occurs as waves that propagate across large areas. Such waves have been observed in the cortex (Garaschuk *et al.* 2000; Corlew *et al.* 2004; Lischalk *et al.* 2009; Conhaim *et al.* 2010), hippocampus (Leinekugel *et al.* 1998), retina (Meister *et al.* 1991), midbrain (Rockhill *et al.* 2009), hindbrain (Gust *et al.* 2003; Hunt *et al.* 2005) and spinal cord (O'Donovan *et al.* 1998). Waves initiated within a particular structure may spread to another structure, such as has been reported between midbrain and hindbrain (Rockhill *et al.* 2009) and between septal nucleus and cortex (Conhaim *et al.* 2010).

Spontaneous activity mediates a large variety of developmental processes. Some of these appear to be intrinsic to single neurons, independent of the patterns of wave propagation, such as neurotrophin gene expression, neuronal migration, and the maturation of ion channel and receptor properties (reviewed in Moody & Bosma, 2005). However, other functions of spontaneous activity depend critically on the spatial and temporal patterns of wave propagation, such as invoking coincidence detection mechanisms to strengthen developing synapses (Kasyanov *et al.* 2004; Voigt *et al.* 2005), conveying the relative spatial location of neuronal somata to their downstream synaptic targets (Shatz & Stryker, 1988), or mediating the change between excitatory and inhibitory GABAergic transmission (Balena & Woodin, 2008).

Spontaneous waves rely on synaptic and intrinsic properties that are specific to developing neurons. The most notable example of this is $GABA_A$ excitation, caused by the high levels of intracellular chloride in developing neurons (Rohrbough & Spitzer, 1996; Owens *et al.* 1996). $GABA_A$ excitation drives spontaneous activity in hippocampus and cortex at some stages of development (Garaschuk *et al.* 1998; Allene *et al.* 2008; present results). Other properties of embryonic neurons are likely to contribute as well, such as high input resistance (Bahrey & Moody, 2003; Picken-Bahrey *et al.* 2003) and high densities of T-type calcium channels (Barish, 1991; Gu & Spitzer, 1993; Tarasenko *et al.* 1998; Biljenga *et al.* 2000).

A central question concerning how spontaneous waves are generated is whether the waves of activity are initiated as an emergent property of the overall circuit (Butts *et al.* 1999) or by a specific population of pacemaker neurons. Although embryonic neural circuits often operate in the parameter space of mutual excitation combined with intrinsic spontaneous activity that can give rise to waves of activity as an emergent property (Butts *et al.* 1999), recent evidence indicates that spontaneous waves in many structures emanate from specific pacemaker regions and/or cell types. Such pacemakers have been identified in hindbrain (Hunt *et al.* 2005), cortex (Lischalk *et al.* 2009; Conhaim *et al.* 2010), retina (Zheng *et al.* 2006) and possibly hippocampus (Strata *et al.* 1997; Leinekugel *et al.* 1998; but see Menendez de la Prida & Sanchez-Andres, 2000).

The pacemaker neurons for each CNS structure are responsible for initiating spontaneous waves during a specific developmental period. The intrinsic and circuit properties of these structures, however, are not static during that period, and the changes in these properties that occur affect both the initiation and propagation of spontaneous waves in ways that are likely to constrain how activity-dependent developmental programs are activated. In cortex, for example, expression of the KCC2 chloride pump in late embryonic and early postnatal neurons results in the gradual conversion of $GABA_A$ action from excitatory to inhibitory throughout the known period of wave generation (Owens *et al.* 1996; Hubner *et al.* 2001). Although the emergence of $GABA_A$ inhibition eventually participates in the termination of cortical spontaneous waves (McCabe *et al.* 2006), it is likely to change the properties of spontaneous waves at earlier stages as well. How it does so will depend critically on the extent to which GABAergic neurons are involved in wave initiation and propagation. A GABAergic pacemaker, for example, would be expected to cease functioning with a modest loss of $GABA_A$ excitation, whereas a glutamatergic pacemaker would require the emergence of substantial $GABA_A$ inhibition at later stages to be prevented from initiating waves of activity.

There are apparently conflicting results as to the transmitter dependence of spontaneous waves in the cortex. It has been reported to be primarily glutamate-based, contrasting with hippocampal activity at the same stages (Garaschuk *et al.* 2000), but also to change form and transmitter dependence from glutamatergic to GABAergic (Allene *et al.* 2008). Other reports indicate participation of both glutamatergic and GABAergic mechanisms even at early stages (Conhaim *et al.* 2010). It would be somewhat surprising if GABAergic mechanisms were not involved at early stages, given evidence that GABA excites cortical neurons and elicits Ca^{2+} transients in both embryonic and early postnatal cortical neurons (Owens *et al.* 1996).

In the present experiments, we used wide-field whole-slice calcium imaging to investigate how the initiation and propagation of waves change during early development, and to determine how those changes relate to the development of GABA and glutamate function in the cortical circuitry. We find that during the period between E18 and P12, cortical waves change from a primarily GABA-based to glutamate-based pacemaker. We also find that the early, GABA-based waves are primarily restricted to the ventral pacemaker regions, possibly accounting

for why GABAergic mechanisms have not always been detected in cortical activity at early stages. Later, glutamate-based waves propagate throughout the cortex. The transition between GABA- and glutamate-based wave mechanisms may be a compensatory mechanism that operates to ensure that spontaneous waves continue to be generated as GABA becomes inhibitory. These complex changes in transmitter dependence and propagation patterns are likely to increase the information content of waves and enable them to carry out more complex developmental functions.

Methods

Ethical approval

All procedures involving animals in this study were approved by the Institutional Animal Care and Use Committee (IACUC) at the University of Washington, following guidelines established by Association for Assessment and Accreditation of Laboratory Animal Care International (AALAC).

Animals

Time-mated Swiss–Webster mice were purchased from Harlan (Indianapolis, IN, USA). Pregnant females were killed on gestational day 17 (E17) by trained personnel using CO_2 inhalation followed by decapitation. Fetuses were removed from the uteri, decapitated and brains placed into ice-cold artificial cerebrospinal fluid (ACSF; see below) equilibrated with carbogen gas (95% O_2–5% CO_2).

Slice preparation and culture

Brains were mounted in the holder of a vibratome (TPI, St Louis, MO, USA). Coronal slices (300–400 μm) were taken from the region anterior to the hippocampus, but within the extent of the lateral ventricles (corresponding approximately to gestational day 18 coronal sections 8–10 in Schambra *et al.* 1992). These sections include cortex, corpus callosum, septal nuclei and basal ganglia structures (caudate-putamen and globus pallidus). Slices were placed on Millicell sterilized culture plate inserts (Millipore Corp., Billerica, MA, USA) in 1 ml of culture medium (see below), and cultured in a water-jacketed incubator at 36–37°C in 5% CO_2. Previous experiments have shown that cultured slices reproduce the time course of several physiological properties of cortical neurons (voltage-gated sodium and potassium currents, capacitance, resting conductance), the onset and disappearance of spontaneous waves (McCabe *et al.* 2006) and the dorsal migration of GABAergic interneurons (C. R. Easton & W. J. Moody, unpublished observations).

Solutions

Cell culture medium contained 75% sterile Neurobasal-A Medium (1X) (Invitrogen, Carlsbad, CA, USA), 25% horse serum (Sigma), penicillin (100 IU ml^{-1}), streptomycin (0.1 mg ml^{-1}) and 2 mM L-glutamine (HyClone Laboratories Inc., Logan, UT, USA). Artificial cerebrospinal fluid contained (mM): 140 NaCl, 3 KCl, 2 $MgCl_2$, 2 $CaCl_2$, 1.25 $NaHPO_4$, 26.5 $NaHCO_3$ and 20 D-glucose. Picrotoxin and CNQX (Tocris) were used at 10 μM and 25 μM, respectively, in ACSF.

Calcium imaging

Cultured tissue slices were removed from the incubator and held in oxygenated ACSF at 30°C for 1–2 h. Slices were then immersed in oxygenated ACSF containing the $[Ca^{2+}]_i$-indicating dye Fluo-4 (1.5 μM) and 0.07% Pluronic F-127 (Molecular Probes, Eugene, OR, USA) for 30–45 min, rinsed and placed into a glass-bottomed experimental chamber. Oxygenated ACSF (30–34°C) was superfused continuously during experiments. Images were captured at an interval of 0.75 s with CoolSnap ES or QuantEM512SC cameras (Photometrics, Tucson, AZ, USA) attached to a Nikon AZ100 microscope. Images were recorded using either MetaFluor (Universal Imaging, West Chester, PA, USA) or NIS Elements AR software (Nikon USA, Melville, NY, USA).

Immunocytochemistry

Calcium-imaged slices were fixed in 4% paraformaldehyde (PFA), rinsed with phosphate buffered saline (PBS), then treated with primary antibody (rabbit α GAD65/67, 1:500, US Biological) and 10% normal goat serum (NGS) in PBS plus 1% Triton X-100 (PBST). Slices were rinsed again in PBS, and secondary antibody (goat α rabbit 594, 1:400, Invitrogen) applied with 10% NGS in PBST. PFA, primary and secondary antibodies were all applied overnight, and PBS rinses in between these applications consisted of 5 rinses of 15–20 min duration. A Texas Red filter set was used for imaging. Three control slices were calcium imaged, and had secondary antibody applied with no primary antibody before imaging. In all cases bleed-through of remaining calcium signal into the 594 channel was minimal, and little signal was observed. Additional ($n = 15$) E18 and P0 cultured slices were not calcium imaged, and were immunostained following the above procedures. In all cases GAD65/67 immunofluorescence matched what was seen in calcium imaged slices, indicating that our immuno results were not

influenced by bleed-through from the calcium dye in the 488 channel.

Data analysis

Stored image sequences were analysed for event frequencies in various regions by placing regions of interest (ROIs) bilaterally over the septal nuclei, and ventral, lateral and dorsal cortex (see Fig. 1). Using NIS Elements software, mean fluorescence for each ROI *vs.* time was recorded from the image stack and exported into SigmaPlot spreadsheet software (Systat, Chicago). Activity in each slice was displayed in SigmaPlot by stacking the fluorescence records for each ROI in a single plot (e.g. Fig. 3). Frequency and interval data from each ROI was calculated using custom-written MatLab functions. Raw F *vs.* time data from each ROI were imported into MatLab and converted into $\Delta F/F$ records. These records were subjected to an event detection routine based on a $\Delta F/F$ threshold of 0.7–1.0%. For each event detected, the time of its occurrence (peak) and its amplitude were stored in MatLab arrays, which were used to calculate event frequency and event interval distribution. Montages and films of events were created from image stacks using custom-written MatLab functions. Fluorescence image stacks were imported into MatLab, converted into $\Delta F/F$ images, and passed through a linear 5×5 pixel spatial filter to reduce noise and emphasize clusters of active pixels. The frames were then thresholded at 3 standard deviations (SD) above mean background fluorescence, and the resulting activity pseudocoloured and superimposed onto a camera image of the slice so that the pathway of wave spread could be visualized in relation to slice anatomy. This superposition was done by scaling down the pixel values of the camera image and blanking those portions of the image under the activity, so as to preserve accurate $\Delta F/F$ values for the events. The speed of wave propagation in the ventral cortex near the point of initiation is rapid compared to our frame capture rate, so that accurate points of wave initiation could not be determined for many events. To find initiation points, a MatLab function scanned image stacks for the first frame of each event that contained a contiguous cluster of pixels with densities >3 SD above mean background $\Delta F/F$. Events with an initial frame in which these pixels comprised <1% of the slice area were analysed for the location of this initiation point by measuring the angles bounding the pixel cluster (see Conhaim *et al.* 2010) and the fractional depth between pial surface and slice midpoint of the centroid of the pixel cluster. Analysis of GAD immunofluorescence in different brain regions was done by using the same ROIs as for Fluo-4 signals (Fig. 1). Mean pixel intensity (background subtracted) was calculated for each ROI. To detect the location of edge points of immunofluorescence decline (e.g. Fig. 8), a MatLab function that detects local maxima of the first spatial derivative of fluorescence along the path of wave propagation was used.

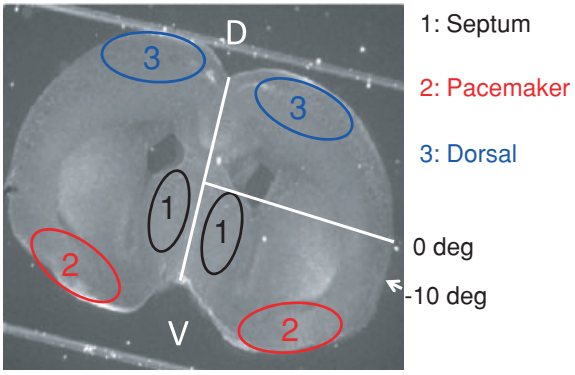

Figure 1. Camera image of a typical cultured coronal slice used in these experiments
White lines indicate the midline of the slice and the 0 deg reference line extending from the midpoint of the midline to the pial surface. Numbered areas indicate the regions of interest (ROIs) used in Fluo-4 fluorescence records presented in the later figures (1: septal nuclei; 2: ventral cortical pacemaker; 3: dorsal cortex follower). The −10 deg label indicates the mean maximum extent of propagation of waves that do not enter the dorsal cortex. Waves that cross this point (fully propagating waves; FPWs) typically reach the dorsal midline, and never stop ventral to +60 deg (Conhaim *et al.* 2010). The same angular reference points were used on both sides of the slice.

Results

In mouse cortex, spontaneous waves at E18–P1 occur as propagating waves that are initiated in a pacemaker in the ventral cortex (ROI 2 in Fig. 1) (Lischalk *et al.* 2009; Conhaim *et al.* 2010). In some waves, this cortical pacemaker is itself triggered by preceding activity in the septal nuclei (ROI 1 in Fig. 1) (Conhaim *et al.* 2010). In both cases, waves of activity propagate dorsally from the site of initiation at rates between 7 and 16 mm s^{-1}. Only 16% of these waves propagate out of the ventral cortex to invade the dorsal cortex. The 84% of waves that are restricted to the pacemaker region stop at a very consistent point near the rhinal fissure, the boundary between piriform cortex (paleocortex) and neocortex (arrow, Fig. 1). Waves that do propagate into the dorsal cortex transiently slow their rate of propagation to 0.5 mm s^{-1} at this same point (see Conhaim *et al.* 2010).

Frequency and patterns of spontaneous waves change with development

To determine the range of stages during which spontaneous waves occur and how wave initiation and propagation change during that period, we used calcium

imaging methods in 272 slices from 163 animals between E18 and P12. We found that propagating waves can be detected in cortex at all stages from E18 to P12 (Fig. 2*A*). At all stages, waves are initiated in either the septal nucleus or the ventral cortex (pacemaker), as we reported for activity at E18–P1 (Conhaim *et al.* 2010). The pattern of wave propagation, however, changes markedly during this period. The frequencies of events in the septal nucleus and pacemaker increase from E18 to peak values at P0 and P2, respectively, and then decrease steadily to near zero at P12 (Fig. 2*A*). The frequency of activity in the dorsal cortex (ROI 3 in Fig. 1) follows a different pattern, starting near zero at E18, rising gradually to peak at P5, and then decreasing to zero at P10. Thus, more events are initiated in the septum and pacemaker regions at early stages, but only a small percentage of those events propagate to the dorsal cortex. As development proceeds past P2, fewer events are initiated, but a greater fraction propagate into the dorsal cortex, so that event frequency in the dorsal cortex increases until P5. After P5, event frequencies in all regions decrease. This relationship is quantified in Fig. 2*B*, which shows the fraction of pacemaker events that propagate into the dorsal cortex as a function of stage. This fraction starts at 7% at E18, and increases steadily to reach 72% at P8. We did not measure significant changes in wave propagation velocity with development.

Sample records of fluorescence *vs.* time for each of the ROIs (see Fig. 1) are shown in Fig. 3. These records illustrate the reciprocal changes in pacemaker and dorsal event frequencies between P0 and P7. Figure 4 shows montages of images from films of Fluo-4 fluorescence superimposed on slice camera images (see Methods) for the two events marked in Fig. 3 at P0 and P7.

Transmitter dependence of spontaneous waves changes with development

The above results show that spontaneous waves occur in cortex during a relatively long period of postnatal development, a time that spans the stages during which cortical GABA action changes from excitatory to inhibitory (Owens *et al.* 1996). Similar waves in hippocampus depend strongly on excitatory GABA transmission (Leinekugel *et al.* 1997), but cortical waves have been reported to depend primarily on AMPA-type glutamatergic activity (Garaschuk *et al.* 2000). We next asked whether the transmitter dependence of cortical waves might change during development, and how the changing nature of GABAergic transmission was manifest in wave properties.

At early stages (E18–P0), picrotoxin, a $GABA_A$ receptor blocker, blocks spontaneous waves by >90%, indicating a strong dependence of spontaneous waves of activity on $GABA_A$ excitation (Fig. 5*A* and *B*). By P6, however, picrotoxin exerts only a 33% block of activity, and by P7, picrotoxin increases the frequency of activity by 1.5-fold, indicating that $GABA_A$ action is inhibitory to waves. After P10, picrotoxin induces waves in slices that were previously silent (Fig. 5*C*), suggesting that the emergence

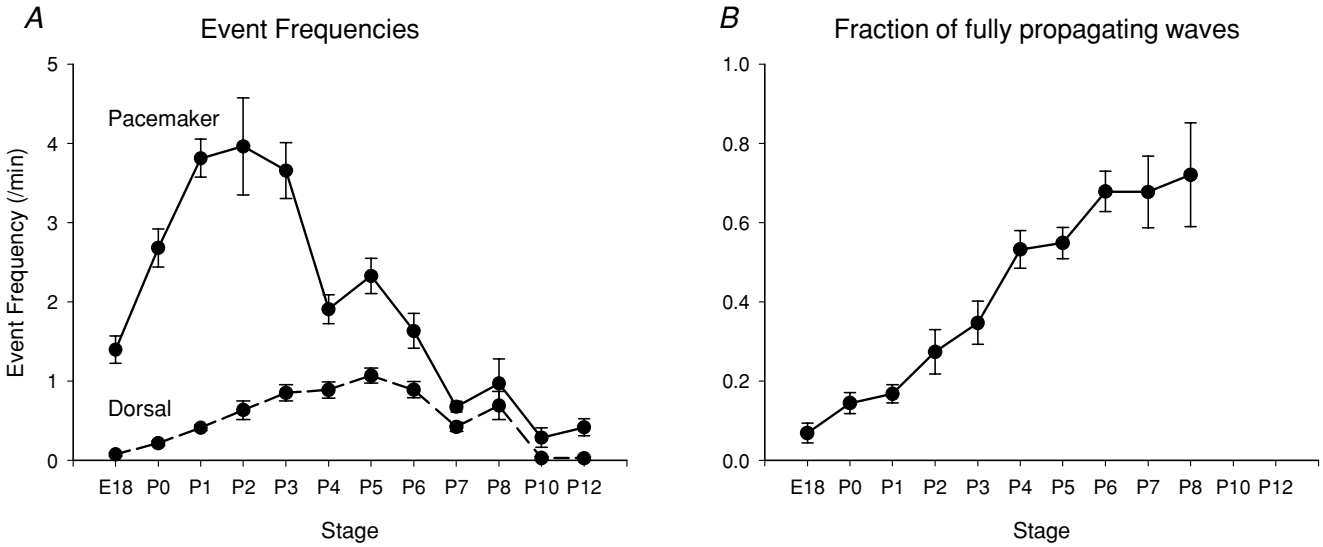

Figure 2. Developmental changes in the frequency and spatial pattern of spontaneous waves
A, frequency of spontaneous waves in the ventral pacemaker (continuous line) and dorsal follower (dashed line) regions of the cortex. Note that pacemaker frequency is higher than follower frequency at early stages, because few events propagate out of the ventral cortex. Frequencies in the septal nuclei showed a similar pattern to that in the pacemaker regions, but peaked at P0. The apparent increase in frequency in the pacemaker between P4 and P5 is not significant ($P = 0.31$). *B*, the fraction of waves that propagate out of the ventral cortex steadily increases as a function of stage. Measurements beyond P8 were difficult due to the low overall frequency of events.

of $GABA_A$-based inhibition is, at least in part, causing the developmental disappearance of spontaneous waves (see also McCabe *et al.* 2006).

We next asked whether glutamate assumes the role of wave initiation after GABA assumes an inhibitory role. At E18, when $GABA_A$ receptor inhibition blocks waves by >90%, the AMPA receptor blocker CNQX reduces the frequency of waves by only 21% (Fig. 6*A* and *B*). By P6, when $GABA_A$ receptor blockade inhibits waves by only 33%, CNQX exerts a 92% block, and after P6, when $GABA_A$ inhibition stimulates waves, CNQX blocks waves completely (Fig. 6*A* and *C*). (CNQX data were not obtained after P8 because wave frequency is too low for reliable data.) At all stages, CNQX reduced the amplitude of the calcium transients, as seen in Fig. 6*B*. There was a significant transient decrease in CNQX sensitivity between P2 and P3 ($P = 0.005$), stages at which the waves are still substantially blocked by picrotoxin. We do not know the cause of this transient change.

The above data indicate that, although spontaneous waves continue to be generated throughout the period E18–P8, the neurons responsible for initiating them gradually shift from the GABAergic to the glutamatergic population. The shift to glutamatergic waves explains how waves of activity continue to occur even after the changing Cl^- gradient has converted GABA to an inhibitory transmitter.

Local and propagating waves show different transmitter dependence

The above data show that the developmental increase in the fraction of spontaneous waves that propagate from the ventral pacemaker into the dorsal cortex parallels

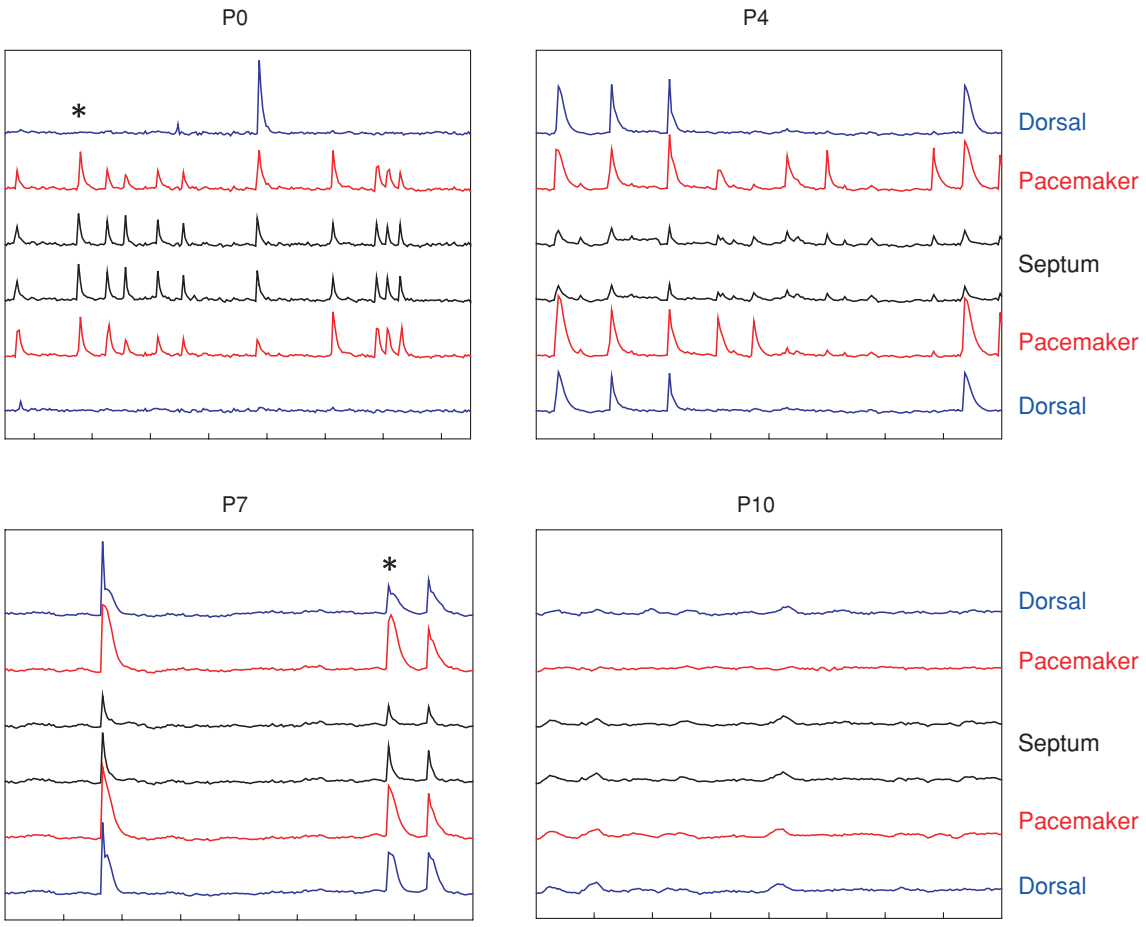

Figure 3. Typical Fluo-4 records of activity at various stages of development
Traces are mean $\Delta F/F$ for the ROIs shown in Fig. 1. Traces are stacked so the regions on the left side of the slice are displayed in the upper half of each graph, those on the right side in the lower half. Moving upward or downward from the centre are septal nuclei (ROIs 1 in Fig. 1), the ventral pacemakers (ROIs 2), and the dorsal follower cortex (ROIs 3). Time markers on the *x*-axes are 20 s for all plots. Traces are stacked at intervals of 1% $\Delta F/F$ in all plots. Note the increasing fraction of waves that propagate into the dorsal cortex between P0 and P7. *Events shown in Fig. 4 films.

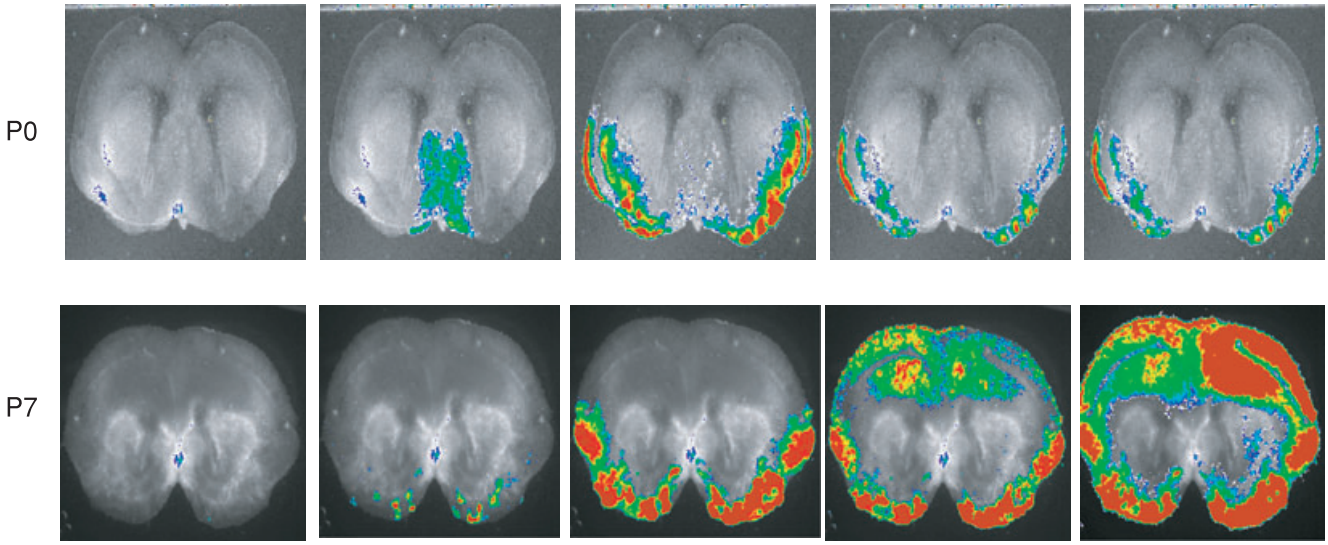

Figure 4. Montages of images of wave propagation at P0 and P7
Events shown are marked in Fig. 3 with asterisks. Fluo-4 fluorescence is displayed (red, high; blue, low in online version) superimposed on the black-and-white slice image (see Methods). Note that the local wave at P0 is initiated in the septal nuclei and stops at a point near 0 deg (see Fig. 1), whereas the P7 wave is initiated in the cortical pacemaker and propagates to the dorsal midline. Both waves were initiated simultaneously on the left and right sides of the slice, which was not always the case. Frame intervals: 0.75 s.

the transition from a GABAergic to a glutamatergic pacemaker (compare Figs 2*B* and 5*A*). This suggests that, at intermediate stages when both transmitter systems participate in spontaneous waves, propagating waves might be mediated by the glutamatergic system and local pacemaker waves by the GABAergic system. To test this hypothesis, we measured the effects of picrotoxin and CNQX on local and fully propagating waves between P1 and P5 (Fig. 7). These results indicate that local waves are approximately seven times more sensitive to picrotoxin

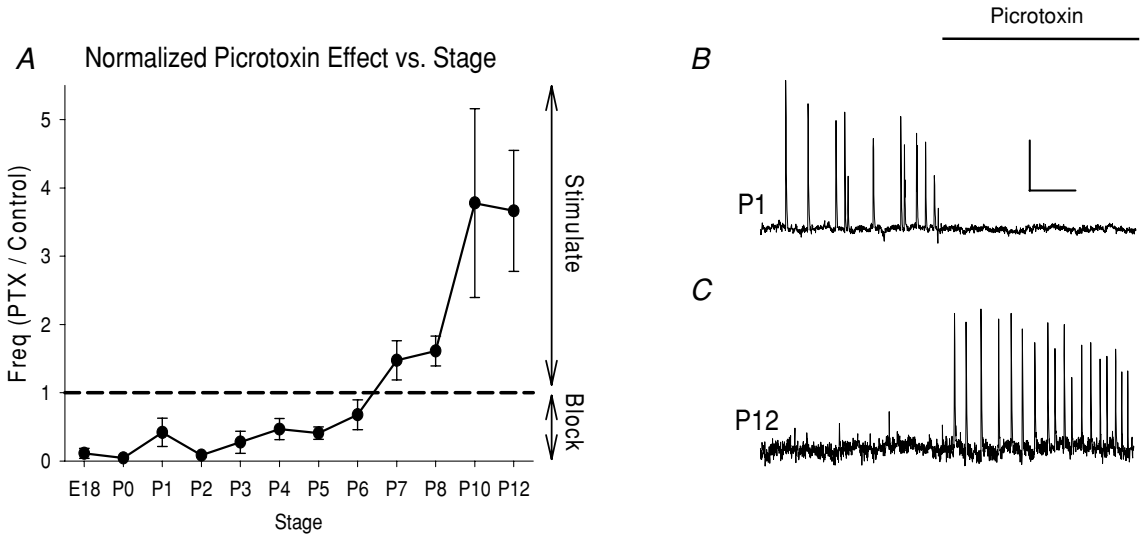

Figure 5. Inversion of the picrotoxin effect on spontanous waves between E18 and P12
A, plot of normalized event frequency in picrotoxin *vs.* control as a function of stage. Numbers <1.0 indicate picrotoxin block of activity; numbers >1.0 indicate that picrotoxin stimulates activity. Dashed line at no picrotoxin effect (1.0) for reference. Note that picrotoxin inhibits activity >90% between E18 and P0, the picrotoxin effect inverts from inhibitory to excitatory between P6 and P7, and picrotoxin stimulates activity after P7. In cases where picrotoxin induced activity in a previously quiescent slice, an arbitrary value of 10 was used. *B*, example of block of spontaneous waves by picrotoxin at P1. *C*, example of induction of spontaneous waves in a previously quiescent slice at P12. In *B* and *C*, activity in the pacemaker is shown (ROI 2 in Fig. 1), although when picrotoxin induced activity at later stages, dorsal regions were also involved in all events. Scale bars: 4 min, 2% $\Delta F/F$.

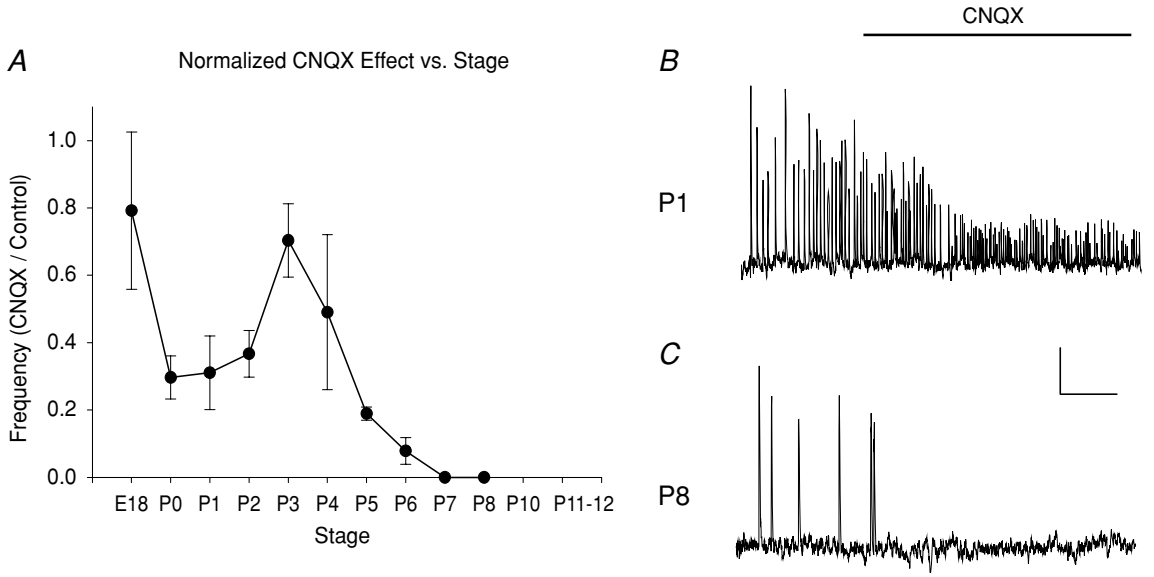

Figure 6. Increase in CNQX block between E18 and P8
A, plot of normalized event frequency in CNQX *vs.* control as a function of stage. Unlike the case for picrotoxin, all numbers are <1.0, because CNQX never stimulates activity. *B*, example of lack of CNQX block of activity at P1. As was typical, CNQX reduced Ca^{2+} transient amplitude, but did not affect frequency. *C*, example of complete CNQX block of activity at P8. In *B* and *C*, activity in the pacemaker is shown (ROI 2 in Fig. 1). Scale bars: 4 min, 2% $\Delta F/F$.

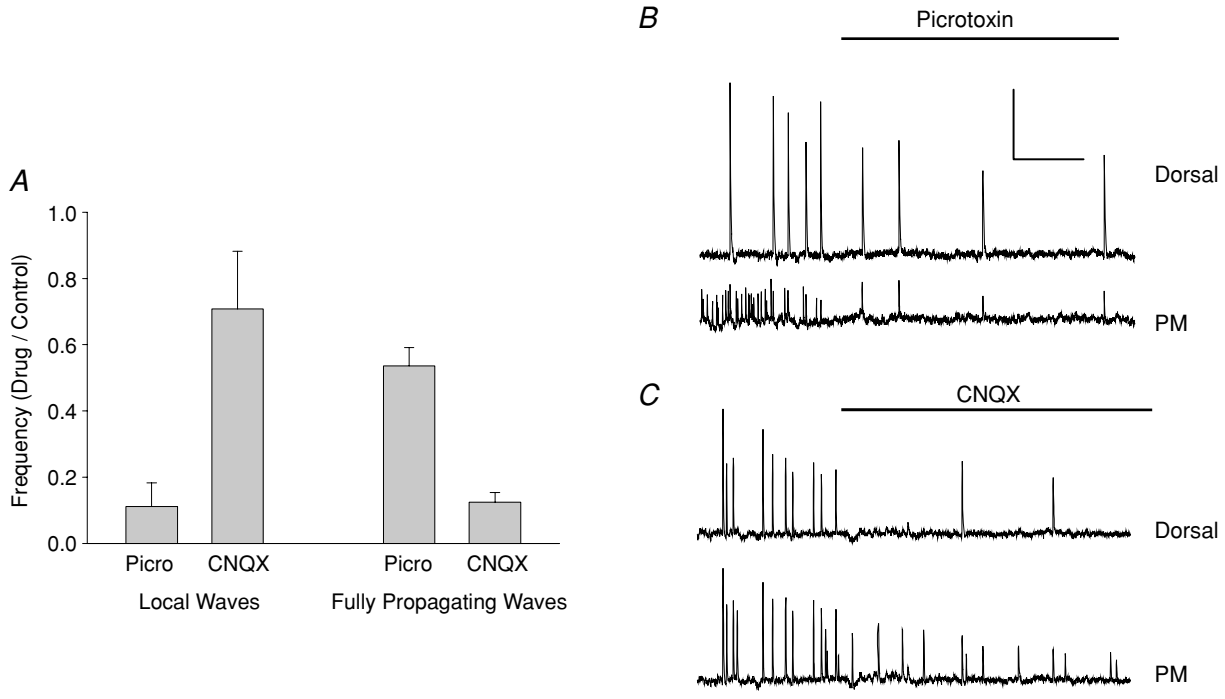

Figure 7. Preferential effects of picrotoxin and CNQX on local and fully propagating waves
A, normalized frequencies of local and fully propagating waves in picrotoxin and CNQX *vs.* control. Picrotoxin preferentially blocks local waves, whereas CNQX preferentially blocks fully propagating waves. Data collected from P1–P5 slices, in which both types of waves showed significant frequencies (see Fig. 2). *B*, picrotoxin effect on activity in a P1 slice. Lower trace is from the pacemaker region (ROI 2 in Fig. 1); upper trace from dorsal region (ROI 3). Note that picrotoxin reduces pacemaker frequency much more than dorsal frequency. *C*, CNQX effect on activity in a P3 slice. Same regions as in *B*. Note that CNQX has the opposite effect, greatly reducing dorsal activity while having little effect on pacemaker frequency. Scale bars: 4 min, 4% $\Delta F/F$.

than are propagating waves (Fig. 7*A* and *B*). Conversely, fully propagating waves are about six times more sensitive to CNQX than are local waves (Fig. 7*A* and *C*). One interpretation of these data is that waves that are initiated by ventral GABAergic neurons do not often propagate dorsally because of the limited number of GABAergic neurons in the dorsal cortex at these stages (see below) and immature synaptic connections between this GABAergic population and dorsal glutamatertic neurons. Later, when ventral glutmatergic neurons become involved in wave initiation, synaptic circuitry within that population might allow more dorsal propagation.

Initiation sites and propagation patterns of spontaneous waves correlate with GABAergic neuron location

The fact the early GABAergic waves are restricted to the ventral cortex may be related to the location of GABAergic neurons themselves, as inhibitory interneurons are born in the ventrally located ganglionic eminences and radiate tangentially to their final destinations in dorsal cortex (Lavdas *et al.* 1999). To test directly whether waves at these stages are localized to regions containing GABAergic neurons, we stained E18 and P0 slices with antibodies directed against the synthetic enzyme for GABA, glutamic acid decarboxylase (GAD65/67; see Methods) ($n = 20$). Figure 8*A* shows a typical staining pattern, with higher expression of GAD65/67 in the septal nuclei and ventral cortex than in dorsal cortex. Within the ventral cortex, GAD expression declined in two steps along the path of wave propagation, one near −45 deg from the horizontal midline (Fig. 8*A*, white arrow) and a second near the boundary between ventral and dorsal cortex near the point of the rhinal fissure (Fig. 8*A*, black arrow). (These steps were detected as local maxima of the first spatial derivative of pixel density along the path of wave propagation. See Methods.) The resulting overall pattern of staining is

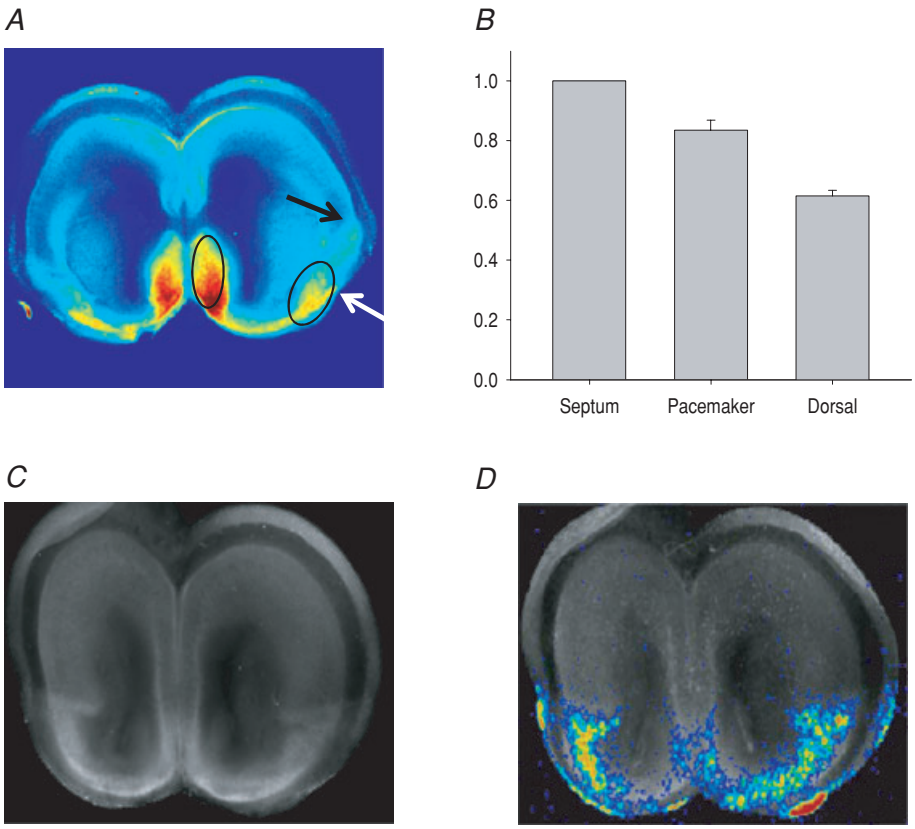

Figure 8. Pattern of GAD 65/67 staining in relation to wave propagation
A, GAD65/67-stained coronal P0 slice. Arrows show two points of drop-off of GAD staining in the path of wave propagation. The second point (black arrow) is near the rhinal fissure and is not significantly different from the point at which local waves stop (see text). The elliptical area comprises 95% of all points of origin of waves. *B*, histogram of mean pixel intensities from all GAD65/67-stained slices (E18–P0) in the same regions as shown in Fig. 1. Staining is highest in the septal nuclei (normalized to 1.0), lower in the pacemaker region (0.83 ± 0.03; $P = 0.005$ *vs.* septum), and lowest in the dorsal follower regions (0.61 ± 0.02; $P < 0.001$ *vs.* both septum and pacemaker). *C*, GAD65/67 staining, showing clear boundary near the rhinal fissure. *D*, Fluo-4 fluorescence at maximum spatial extent of a spontaneous wave in the same slice, superimposed on the GAD65/67 staining. The maximum extent of propagation of the wave is seen to very closely follow the distribution of GAD65/67 staining.

summarized in Fig. 8*B*, in which mean staining intensity is quantified in the same ROIs shown in Fig. 1. GAD staining is highest in the septal nuclei, slightly but significantly lower in the ventral cortex, and lowest in the dorsal cortex. The two elliptical regions in Fig. 8*A* are drawn to encompass 95% of all wave initiation points ($n = 55$) (see Methods), indicating that wave initiation at these stages occurs consistently within regions of high GAD expression.

At these stages, spontaneous waves are mostly restricted to the ventral cortex. To test how closely this stop point corresponds to the second decline in GAD staining (Fig. 8*A*, black arrow), we imaged waves in nine E18–P0 slices and then processed those slices for GAD antibody staining. The second decline in GAD staining was located just ventral to the ventral–dorsal boundary of the slice (-9.9 ± 0.59 deg; see Fig. 1). This was not significantly different from the wave arrest point measured in our overall population of E18–P0 slices (-8.2 ± 0.7 deg, $n = 81$; $P = 0.31$), or within the slices where we obtained both imaging and GAD staining (-7.7 ± 1.0 deg; $n = 9$; $P = 0.07$). The close correspondence of the maximum extent of wave propagation at these early stages with the pattern of GAD staining is emphasized in Fig. 8*C* and *D*, which compares the maximum extent of wave spread with GAD staining in the same slice.

These data indicate that at early stages of development, between E18 and P0, when pharmacological evidence indicates a strong GABAergic component to spontaneous waves, waves initiate in regions of high GAD expression, and the spatial extent of their propagation is limited either by the spatial distribution of GABAergic neurons themselves or by the strength of the synaptic interactions among them, as indicated by elevated GAD expression.

Discussion

Waves of spontaneous activity propagate across both hemispheres of the mouse cerebral cortex from E18 to P12. We have shown that during this period, the waves undergo marked changes in frequency, in the spatial patterns of propagation, and in transmitter dependence. At all of these stages, waves are initiated in one of two pacemaker locations: the septal nuclei or the ventrolateral cortex (Lischalk *et al.* 2009; Conhaim *et al.* 2010). Frequencies of activity in these two regions peak at P0 and P2, respectively. At E18 and P0, about 90% of the waves are restricted to the septal nucleus and ventral cortex, with only 10% crossing into the dorsal cortex to reach the dorsal midline. As development proceeds, an increasing fraction of waves propagate dorsally, so that by P4, half of all waves propagate dorsally and by P8, 75% do. During these later stages, the frequency at which waves are initiated by the septal nucleus and ventral cortical pacemaker gradually decreases, so that the absolute frequency of waves propagating into the dorsal cortex peaks at P5 (Fig. 2).

All of our experiments were done in coronal slices. Spontaneous activity has also been recorded in horizontal slices, in which wave propagation in the anterior–posterior direction has been reported (Garaschuk *et al.* 2000; Corlew *et al.* 2004). It is likely that the 3-dimensional propagation patterns *in vivo* are more complex than either section plane reveals, which may increase the information content of the waves beyond what we detect here.

As these changes in the spatial patterns of propagation occur, the waves also change their transmitter dependence. At early stages, when most waves are local to the septal nucleus and ventral cortex, waves are blocked completely by picrotoxin but only partially by CNQX, indicating that wave initiation is primarily a function of GABAergic neurons. As development proceeds and an increasing fraction of waves propagate dorsally, picrotoxin sensitivity gradually diminishes and CNQX sensitivity increases, indicating a switch in the neuronal populations that initiate waves from GABAergic to glutamatergic (Figs 5 and 6). At intermediate stages, when both transmitter systems are participating, local waves are preferentially blocked by picrotoxin whereas propagating waves are preferentially blocked by CNQX (Fig. 7). These data and the immunocytochemical evidence shown in Fig. 8 indicate that developmental changes in wave propagation are a function of changing transmitter dependence and the different spatial distribution of GABAergic and glutamatergic neuronal populations.

Emergence of glutamatergic pacemaker parallels loss of GABA excitation

By P7, glutamatergic transmission assumes the primary role for initiating and propagating spontaneous waves and GABA becomes inhibitory to their initiation, as evidenced by the inversion of the picrotoxin effect on wave frequency from inhibitory to stimulatory at this stage (Fig. 5). The emergence of the cortical glutamatergic pacemaker, therefore, allows spontaneous waves to continue despite the changing sign of GABA action. Our data also indicate that glutamatergic circuits play a major role in causing waves to propagate into the dorsal cortex at later stages (see Fig. 7). The biological role of the switch in transmitter dependence of the cortical pacemaker may be to allow spontaneous waves to span a range of critical developmental stages that extend beyond the time when GABA transmission becomes inhibitory and incapable of wave initiation. Presumably, the cessation of waves after P12 reflects the development of GABA inhibition that is sufficiently intense to limit spontaneous activity to smaller clusters of coactive

neurons (Rochefort *et al.* 2009) and to override the ability of glutamatergic excitation to initiate and propagate waves.

The transition in GABA action on spontaneous waves between P6 and P7 does not necessarily indicate that GABA becomes inhibitory as judged by the effects of its application to inactive cortical neurons. In order to inhibit the generation of waves, GABA action need only reduce the level of glutamatergic excitation to a point where it cannot sustain waves of activity, an action that GABA could carry out when its reversal potential becomes sufficiently negative to the glutamate reversal potential, even if it were still positive to threshold. Thus, it is possible for GABA to excite inactive neurons while at the same time inhibiting circuit generation of waves.

This switch in transmitter dependence of spontaneous waves parallels that reported in hippocampus (Garaschuk *et al.* 1998), but contrasts with the change from glutamatergic to GABAergic mechanisms reported in rat cortex (Allene *et al.* 2008) and the purely glutamatergic wave initiation reported by Garaschuk *et al.* (2000), also in rat. There are several possible explanations for these apparent discrepancies. GABA and glutamate have different effects on rat and mouse cortical neuronal migration (Behar *et al.* 1999), raising the possibility of species differences in the mechanisms of spontaneous waves. A more likely possibility, however, is that multiple mechanisms of spontaneous activity coexist in the cortex, as shown directly by Allene *et al.* (2008), and that the location and size of the recording field influences the results obtained. For example, at early stages in mouse cortex, spontaneous waves are restricted to the ventral regions, so that recordings in dorsal areas might show localized patterns of spontaneous activity different from the later waves that enter this region from the ventral pacemaker. Even within the ventral pacemaker, both GABAergic and glutamatergic events can coexist at intermediate stages (see Fig. 7).

In our experiments, the ventrolateral location of the cortical initiation zone does not change during the switch from GABA- to glutamate-based pacemaker. We could not determine the specific location within that ventrolateral region at all stages because wave propagation within the ventral cortex is too fast for our frame capture rate to detect small initiation points consistently (see Conhaim *et al.* 2010), so it remains possible that there is a small shift in pacemaker location as initiation switches between neuronal populations. The question remains, however, as to why the pacemaker remains ventrally located. Glutamatergic neurons are more widespread in the cortex at early stages because of their radial migratory pathway, in contrast to the tangentially migrating GABAergic neurons (Lavdas *et al.* 1999). It appears that some combination of intrinsic and synaptic properties of the glutamatergic circuitry in the ventral cortex endows those neurons with pacemaking ability. One possibility is that ventral glutamatergic neurons acquire these properties because they are exposed to high frequencies of GABA-initiated waves at early stages. If the GABAergic pacemaker activates glutamatergic neurons synchronously in this region, coincidence-detection mechanisms are likely to be invoked that strengthen glutamatergic synapses to the point that they form functional circuits capable of wave initiation. In this model, the shift to glutamatergic waves would depend on preceding GABAergic waves.

In fact, the close correspondence at early stages between GAD immunofluorescence and wave boundaries might also reflect activity-dependent mechanisms, especially of GAD-67 expression (Huang, 2009). It is possible that a feedback loop exists at early stages of cortical waves, whereby initial ventral localization of GABAergic neurons drives ventrally restricted waves, which in turn up-regulate GAD expression and strengthen synaptic transmission among GABAergic neurons within that restricted area, keeping wave localization relatively constant even as GABAergic interneurons continue to migrate dorsally.

Complex information content of variably propagating waves

These patterns endow spontaneous waves with a high level of information content compared to waves with uniform frequency and spatial patterns of propagation. Consider, for example, the differences between activity experienced by neurons in the dorsal *vs.* ventral cortex. In the dorsal cortex, activity at all stages will be correlated with immediately preceding activity ventrally, because all waves are initiated by the ventrally located pacemaker. However, as development proceeds between E18 and P10, dorsal and ventral neurons experience very different patterns of activity. Ventral neurons experience high frequencies of activity at early stages, and then frequency decreases gradually beginning at P2. Dorsal neurons, on the other hand, initially experience very low frequencies of activity because only a small fraction of waves propagate into the dorsal cortex. This frequency increases to a peak at P5, but this peak frequency is only 25% of the earlier peak frequency ventrally. After P5, dorsal and ventral neurons experience about the same, declining frequencies of activity. This suggests that downstream synaptic targets, for example, cannot only detect the spatial relationship between cortical neurons by the intervals between their bursts of activity during individual waves (resulting from the rate of wave propagation), but that they can also detect gross regional location of cortical neurons by the absolute frequencies of their activity at different stages of development.

References

Allene C, Cattani A, Ackman JB, Bonifazi P, Aniksztejn L, Ban-Ari Y & Cossart R (2008). Sequential generation of two distinct synapse-driven network patterns in developing neocortex. *J Neurosci* **28**, 12851–12863.

Bahrey HP & Moody WJ (2003). Voltage-gated currents, dye and electrical coupling in the embryonic mouse neocortex. *Cereb Cortex* **13**, 239–251.

Balena T & Woodin MA (2008). Coincident pre- and postsynaptic activity downregulates NKCC1 to hyperpolarize E_{Cl} during development. *Eur J Neurosci* **27**, 2402–2412.

Barish ME (1991). Increases in intracellular calcium ion concentration during depolarization of cultured embryonic *Xenopus* spinal neurones. *J Physiol* **444**, 545–565.

Behar TN, Scott CA, Greene CL, Wen X, Smith SV, Maric D, Liu QY, Colton CA & Barker JL (1999). Glutamate acting at NMDA receptors stimulates embryonic cortical neuronal migration. *J Neurosci* **19**, 4449–4461.

Biljenga P, Liu JH, Espinaos E, Haenggeli CA, Fischer-Lougheed J, Bader C & Bernheim L (2000). T-type α1H Ca^{2+} channels are involved in Ca^{2+} signaling during terminal differentiation (fusion) of human myoblasts. *Proc Natl Acad Sci U S A* **97**, 7627–7632.

Blankenship AG & Feller MB (2010). Mechanisms underlying spontaneous patterned activity in developing neural circuits. *Nat Rev Neurosci* **11**, 18–29.

Butts DA, Feller MB, Shatz CJ & Rokhsar DS (1999). Retinal waves are governed by collective network properties. *J Neurosci* **19**, 3580–3593.

Conhaim J, Cedarbaum ER, Barahimi M, Moore JG, Becker MI, Gleiss H, Kohl C & Moody WJ (2010). Bimodal septal and cortical triggering and complex propagation patterns of spontaneous waves of activity in the developing mouse cerebral cortex. *Dev Neurobiol* **70**, 679–692.

Corlew R, Bosma MM & Moody WJ (2004). Spontaneous, synchronous electrical activity in neonatal mouse cortical neurons. *J Physiol* **560**, 377–390.

Garaschuk O, Hanse E & Konnerth A (1998). Developmental profile and synaptic origin of early network oscillations in the CA1 region of rat neonatal hippocampus. *J Physiol* **507**, 219–236.

Garaschuk O, Linn J, Eilers J & Konnerth A (2000). Large-scale oscillatory calcium waves in the immature cortex. *Nat Neurosci* **3**, 452–459.

Gu X & Spitzer NC (1993). Low-threshold Ca^{2+} current and its role in spontaneous elevations of intracellular Ca^{2+} in developing *Xenopus* neurons. *J Neurosci* **13**, 4936–4948.

Gust J, Wright JJ, Pratt EB & Bosma MM (2003). Development of synchronized activity of cranial motor neurons in the segmented embryonic mouse hindbrain. *J Physiol* **550**, 123–133.

Huang ZJ (2009). Activity-dependent development of inhibitory synapses and innervation pattern: role of GABA signalling and beyond. *J Physiol* **587**, 1881–1888.

Hubner CA, Stein V, Harmans-Borgmeyer I, Meyer T, Ballanyi K & Jentsch TJ (2001). Disruption of KCC2 reveals an essential role of K-Cl cotransport in early synaptic inhibition. *Neuron* **30**, 515–524.

Hunt PN, McCabe AK & Bosma MM (2005). Midline serotonergic neurons contribute to widespread synchronous activity in embryonic mouse hindbrain. *J Physiol* **566**, 807–819.

Kasyanov AM, Safiulina VF, Voronin LL & Cherubini E (2004). GABA-mediated giant depolarizing potentials as coincidence detectors for enhancing synaptic efficacy in the developing hippocampus. *Proc Natl Acad Sci U S A* **101**, 5311–5312.

Lavdas AA, Grigoriou M, Pachnis V & Parnavelas JG (1999). The medial ganglionic eminence gives rise to a population of early neurons in the developing cerebral cortex. *J Neurosci* **99**, 7881–7888.

Leinekugel X, Khalilov I, Ben-Ari Y & Khazipov R (1998). Giant depolarizing potentials: the septal pole of the hippocampus paces the activity of the developing intact septohippocampal complex *in vitro*. *J Neurosci* **18**, 6349–6357.

Leinekugel X, Medina I, Khalilov I, Ben-Ari Y & Khazipov R (1997). Ca^{2+} oscillations mediated by the synergistic excitatory actions of $GABA_A$ and NMDA receptors in the neonatal hippocampus. *Neuron* **18**, 243–255.

Lischalk JW, Easton CR & Moody WJ (2009). Bilaterally propagating waves of spontaneous activity arising from discrete pacemakers in the neonatal mouse cerebral cortex. *Dev Neurobiol* **69**, 407–414.

McCabe AK, Chisholm SL, Picken-Bahrey HL & Moody WJ (2006). The self-regulating nature of spontaneous synchronized activity in developing mouse cortical neurones. *J Physiol* **577**, 155–167.

Meister M, Wong ROL, Baylor DA & Shatz CJ (1991). Synchronous bursts of action potentials in ganglion cells of the developing mammalian retina. *Science* **252**, 939–943.

Menendez de la Prida I & Sanchez-Andres JV (2000). Heterogeneous populations of cells mediate spontaneous synchronous bursting in the developing hippocampus through a frequency-dependent mechanism. *Neuroscience* **97**, 227–241.

Moody WJ & Bosma MM (2005). Ion channel development, spontaneous activity, and activity-dependent development in nerve and muscle cells. *Physiol Rev* **85**, 883–941.

O'Donovan MJ, Chub N & Wenner P (1998). Mechanisms of spontaneous activity in developing spinal networks. *J Neurobiol* **37**, 131–145.

Owens DF, Boyce LH, Davis MBE & Kriegstein AR (1996). Excitatory GABA responses in embryonic and neonatal cortical slices demonstrated by gramicidin perforated-patch recordings and calcium imaging. *J Neurosci* **16**, 6414–6423.

Picken-Bahrey HP, Albrieux M & Moody WJ (2003). Early development of voltage-gated ion currents and firing properties in neurons of the mouse cerebral cortex. *J Neurophysiol* **89**, 1761–1773.

Rockhill W, Kirkman JL & Bosma MM (2009). Spontaneous activity in the developing mouse midbrain driven by an external pacemaker. *Dev Neurobiol* **69**, 689–704.

Rochefort NL, Garaschuk O, Milos RI, Narushima M, Marandi N, Pichler B, Kovalchuk Y & Konnerth A (2009). Sparsification of neuronal activity in the visual cortex at eye-opening. *Proc Natl Acad Sci U S A* **106**, 15049–15054.

Rohrbough J & Spitzer NC (1996). Regulation of intracellular Cl^- levels by Na^+-dependent Cl^- cotransport distinguishes depolarizing from hyperpolarizing $GABA_A$ receptor-mediated responses in spinal neurons. *J Neurosci* **16**, 82–91.

Schambra UB, Lauder JM & Silver J (eds) (1992). *Atlas of the Prenatal Mouse Brain.* Academic Press Inc., New York.

Shatz CJ & Stryker MP (1988). Prenatal tetrodotoxin infusion blocks segregation of retinogeniculate afferents. *Science* **242**, 87–89.

Strata F, Atzori M, Molnar M, Ugolini G, Tempia F & Cherubini E (1997). A pacemaker current in dye-coupled hilar interneurons contributes to the generation of giant GABAergic potentials in developing hippocampus. *J Neurosci* **17**, 1435–1446.

Tarasenko AN, Isaev DX, Eremin AV & Kostyuk PG (1998). Developmental changes in the expression of low-voltage-activated Ca^{2+} channels in rat visual cortical neurones. *J Physiol* **509**, 385–394.

Voigt T, Optiz T & de Lima AD (2005). Activation of early silent synapses by spontaneous synchronous network activity limits the range of neocortical connections. *J Neurosci* **25**, 4604–4615.

Zheng J, Lee S & Zhou ZJ (2006). A transient network of intrinsically bursting starburst amacrine cells underlies the generation of retinal waves. *Nat Neurosci* **9**, 363–371.

Author contributions

The experiments were carried out in the laboratory of W.J.M. All authors contributed to the design and execution of experiments, to the analysis and interpretation of data, and to the critical revising of the manuscript. W.J.M. drafted the manuscript. All authors approved the final version.

Acknowledgements

This work was supported by grants from the National Science Foundation and the National Institutes of Health to W.J.M. C.R.E. was supported by the NIH Neurobiology Training Grant to the University of Washington, and in part by funding from the NIH to A. Folch, Dept of Bioengineering. M.B., E.R.C., J.G.M. and L.F.M. were supported by the Mary Gates Endowment for Undergraduate Research at the University of Washington.

Chapter Two

Genetic elimination of GABAergic neurotransmission reveals two distinct pacemakers for spontaneous waves of activity in the developing mouse cortex.

Easton CR, Weir K, Scott A, Moen SP, Barger Z, Folch A, Hevner RF, Moody WJ.

(2014)

Journal of Neuroscience
Mar 12;34(11):3854-63.

Genetic Elimination of GABAergic Neurotransmission Reveals Two Distinct Pacemakers for Spontaneous Waves of Activity in the Developing Mouse Cortex

Curtis R. Easton,[1,4] Keiko Weir,[1] Adina Scott,[1] Samantha P. Moen,[1] Zeke Barger,[1] Albert Folch,[2] Robert F. Hevner,[3,4] and William J. Moody[1]

[1]Department of Biology, [2]Department of Bioengineering, and [3]Department of Neurological Surgery, University of Washington, Seattle, Washington 98195, and [4]Center for Integrative Brain Research, Seattle Children's Research Institute, Seattle, Washington 98101

Many structures of the mammalian CNS generate propagating waves of electrical activity early in development. These waves are essential to CNS development, mediating a variety of developmental processes, such as axonal outgrowth and pathfinding, synaptogenesis, and the maturation of ion channel and receptor properties. In the mouse cerebral cortex, waves of activity occur between embryonic day 18 and postnatal day 8 and originate in pacemaker circuits in the septal nucleus and the piriform cortex. Here we show that genetic knock-out of the major synthetic enzyme for GABA, GAD67, selectively eliminates the picrotoxin-sensitive fraction of these waves. The waves that remain in the GAD67 knock-out have a much higher probability of propagating into the dorsal neocortex, as do the picrotoxin-resistant fraction of waves in controls. Field potential recordings at the point of wave initiation reveal different electrical signatures for GABAergic and glutamatergic waves. These data indicate that: (1) there are separate GABAergic and glutamatergic pacemaker circuits within the piriform cortex, each of which can initiate waves of activity; (2) the glutamatergic pacemaker initiates waves that preferentially propagate into the neocortex; and (3) the initial appearance of the glutamatergic pacemaker does not require preceding GABAergic waves. In the absence of GAD67, the electrical activity underlying glutamatergic waves shows greatly increased tendency to burst, indicating that GABAergic inputs inhibit the glutamatergic pacemaker, even at stages when GABAergic pacemaker circuitry can itself initiate waves.

Key words: **activity-dependent development; GABA; pacemaker; piriform cortex; spontaneous activity**

Introduction

Waves of spontaneous electrical activity and associated increases in cellular calcium levels propagate across many structures of the mammalian CNS during early development and are necessary for developmental processes including neuronal differentiation and the refinement of synaptic connections (Moody and Bosma, 2005; Blankenship and Feller, 2010). In many cases, these waves are initiated by specific pacemaker circuits that, depending on the structure, are composed of GABAergic, glutamatergic, serotonergic, or cholinergic neurons (Wong et al., 2000; Hunt et al., 2006; Zheng et al., 2006; Lischalk et al., 2009; Conhaim et al., 2011). In any given structure, complex interactions among the component pacemaker circuits make it difficult to unravel the contributions of each transmitter system to wave initiation. For example, the identity of the initiating circuit may change during development, and homeostatic mechanisms may upregulate one component of the pacemaker when another is blocked (Chub and O'Donovan, 1998; Wong et al., 2000; Conhaim et al., 2011).

In the mouse cerebral cortex, spontaneous waves occur in the early postnatal period and are initiated by pacemaker circuits within the piriform cortex and septal nucleus (Garaschuk et al., 2000; Corlew et al., 2004; Conhaim et al., 2010). These waves are sensitive to blockers of $GABA_A$ and AMPA receptors, but the exact roles of these two transmitter systems in wave initiation remain unresolved (Conhaim et al., 2011). Because many activity-dependent developmental processes rely on information contained in wave frequencies and propagation patterns, understanding the mechanisms that initiate waves and regulate these parameters is critical.

In this study, we eliminate GABAergic transmission by knock-out (KO) of the 67 kDA glutamic acid decarboxylase enzyme (GAD67), which accounts for ≥90% of the brain's production of GABA (Asada et al., 1997; Tamamaki et al., 2003). From analysis of wave activity in brain slices from KO and control animals recorded with calcium imaging and microfluidic-based extracellular arrays, we provide evidence that two semi-independent initiation circuits drive spontaneous waves in the developing cortex. One of these pacemakers uses GABA excitation, resides in the septal nucleus and the piriform cortex, and initiates waves that

Received Sept. 5, 2013; revised Jan. 28, 2014; accepted Jan. 30, 2014.

Author contributions: C.R.E., K.W., Z.B., R.F.H., and W.J.M. designed research; C.R.E., K.W., A.S., S.P.M., Z.B., and W.J.M. performed research; A.F. and R.F.H. contributed unpublished reagents/analytic tools; C.R.E., K.W., A.S., and W.J.M. analyzed data; C.R.E., K.W., and W.J.M. wrote the paper.

This work was supported by National Science Foundation IOB0718344 to W.J.M., National Institutes of Health to A.F., National Institutes of Health Neurobiology Training Grant to C.R.E., and the Mary Gates Endowment for Undergraduate Research to K.W. and S.P.M.

The authors declare no competing financial interests.

Correspondence should be addressed to Dr. William J. Moody, Department of Biology, University of Washington, Seattle, WA 98195. E-mail: profbill@u.washington.edu.

DOI:10.1523/JNEUROSCI.3811-13.2014

 0270-6474/14/343854-10$15.00/0

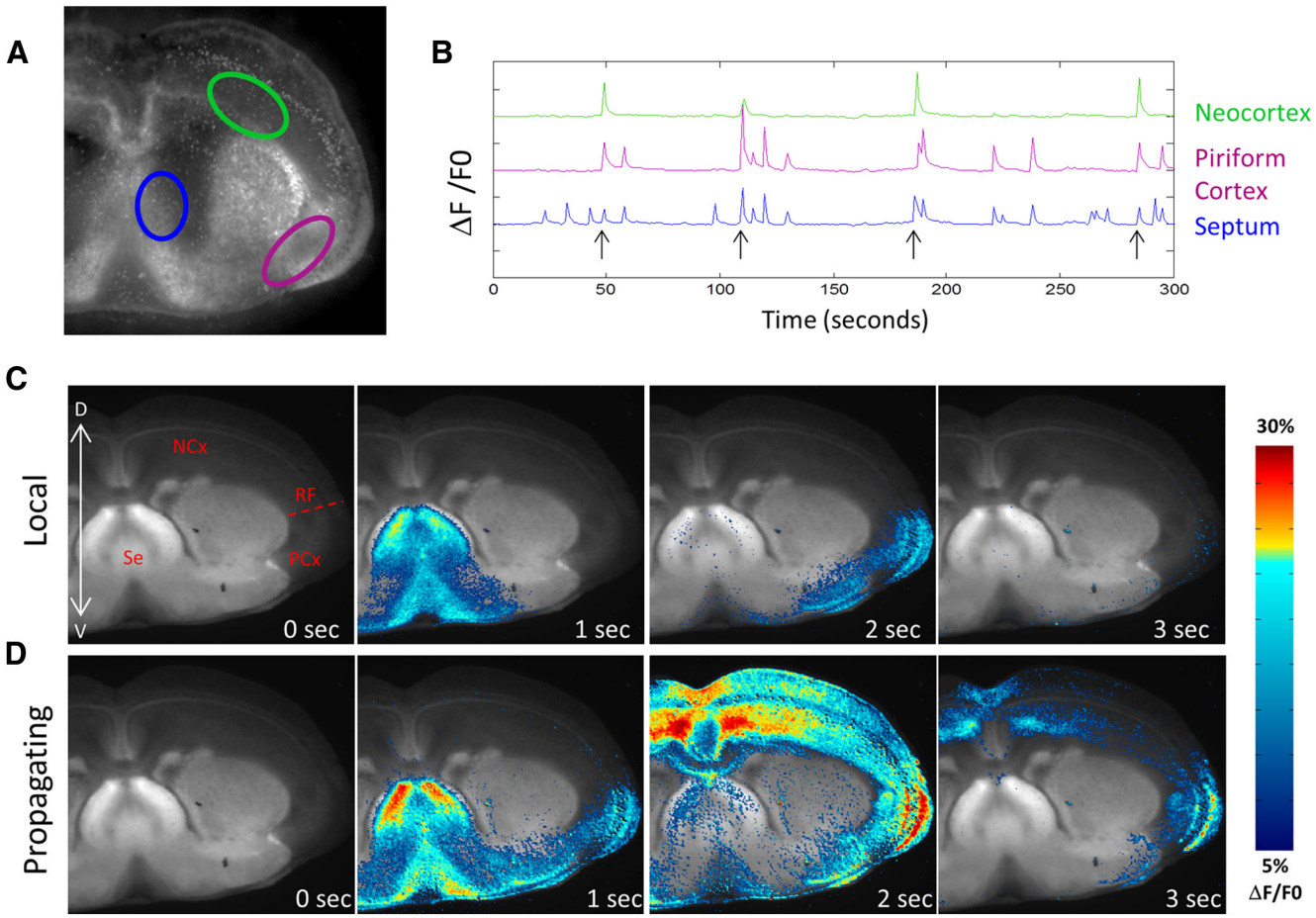

Figure 1. Local and propagating spontaneous waves in mouse cortex. ***A***, Rhod 3 fluorescence image of a coronal slice of mouse brain at P0. ROIs are indicated in the septal nucleus (blue), the piriform cortex (purple), and the neocortex (green). ***B***, Calcium records of mean fluorescence (ΔF/F0) in each ROI showing both local and propagating waves. Propagating waves are indicated by arrows and can be distinguished from local waves by the presence of signal in the neocortex. *y*-axis tick marks indicate 10% ΔF/F0. ***C***, Montage of images taken during a local wave. This wave initiates in the septal nucleus and enters the piriform cortex but does not propagate dorsally into the neocortex. Structures labeled in the first frame: NCx, Neocortex; RF, rhinal fissure; PCx, piriform cortex; Se, septal nuclei. ***D***, Montage of images taken during a wave that propagates into the neocortex and, in this case, crosses the midline into the contralateral neocortex. ***C***, ***D***, Images were created by thresholding the calcium signal, applying to it a color map, and then superimposing the colored ΔF/F0 signal onto a grayscale image showing GFP distribution in the slice. See Materials and Methods.

have a low probability of propagating into the neocortex. The other pacemaker uses glutamatergic circuitry, resides primarily in the piriform cortex, and preferentially initiates waves that invade the neocortex. The selective developmental sparing of the glutamatergic pacemaker in the chronic absence of the GABAergic system indicates that the emergence of the glutamatergic pacemaker does not require GABAergic waves and that glutamatergic waves do not increase their frequency to compensate for the absence of the GABAergic waves.

The structures that contain these two pacemakers (the septal nucleus and the piriform cortex) develop earlier than the neocortex and have extensive connections with it. The existence of two wave initiation systems within these structures may allow spontaneous waves of activity to enter the neocortex before it is developmentally mature enough to initiate them. The sequential participation of both GABAergic and glutamatergic neurons in wave initiation may provide timing cues for the coordinated maturation of the inhibitory and excitatory circuitry of the cortex.

Materials and Methods

Animal procedures. Time-mated females carrying E17 fetuses were killed with carbon dioxide, and the fetuses were removed and placed on ice. Brains were removed from the fetuses and sliced 300 μm thick in ice-cold ACSF using a Leica VT1200S vibrating microtome. All animal procedures were approved by the Institutional Animal Care and Use Committee at the University of Washington.

Generation of GAD67 KO mice. We used a GAD67-GFP knock-in line (Tamamaki et al., 2003) as the basis for eliminating GAD67 genetically. GAD67-GFP homozygous KO embryos (*GAD67 KO*) were obtained by crossing males and females both heterozygous for GAD67-GFP. Homozygous embryos were identified by first visually identifying embryos with GFP expression and then selecting the subset of those embryos that also expressed cleft palate, a marker for *GAD67 KO* (Asada et al., 1997). The classification of embryos was confirmed by PCR. GAD67-GFP heterozygotes were used as controls and were obtained by crossing *CD1-WT* females with *GAD67-GFP* heterozygous male breeders. *GAD67-GFP* heterozygous embryos were identified by GFP expression.

Slice cultures. Coronal slices were taken from E17 fetuses at a position anterior to the hippocampus and posterior to the olfactory bulbs, where the lateral ventricles were clearly visible. Slices were interface-cultured on Millicell 0.4 μm, 30 mm culture inserts (Millipore) in medium composed of 75% sterile Neurobasal-A Medium (1×) (Invitrogen), 25% horse serum (Sigma), penicillin (100 IU/ml), streptomycin (0.1 mg/ml), and 2 mM L-glutamine (HyClone Laboratories). Although penicillin is a known epileptogenic agent in slices, the concentrations used in that context are 3- to 20-fold higher than in our culture medium (Schneiderman, 1986). In addition, we find similar activity in acute slices that have never been exposed to penicillin. Slices were cultured for 2–5 d and then removed from the incubator and placed into ACSF for physiological re-

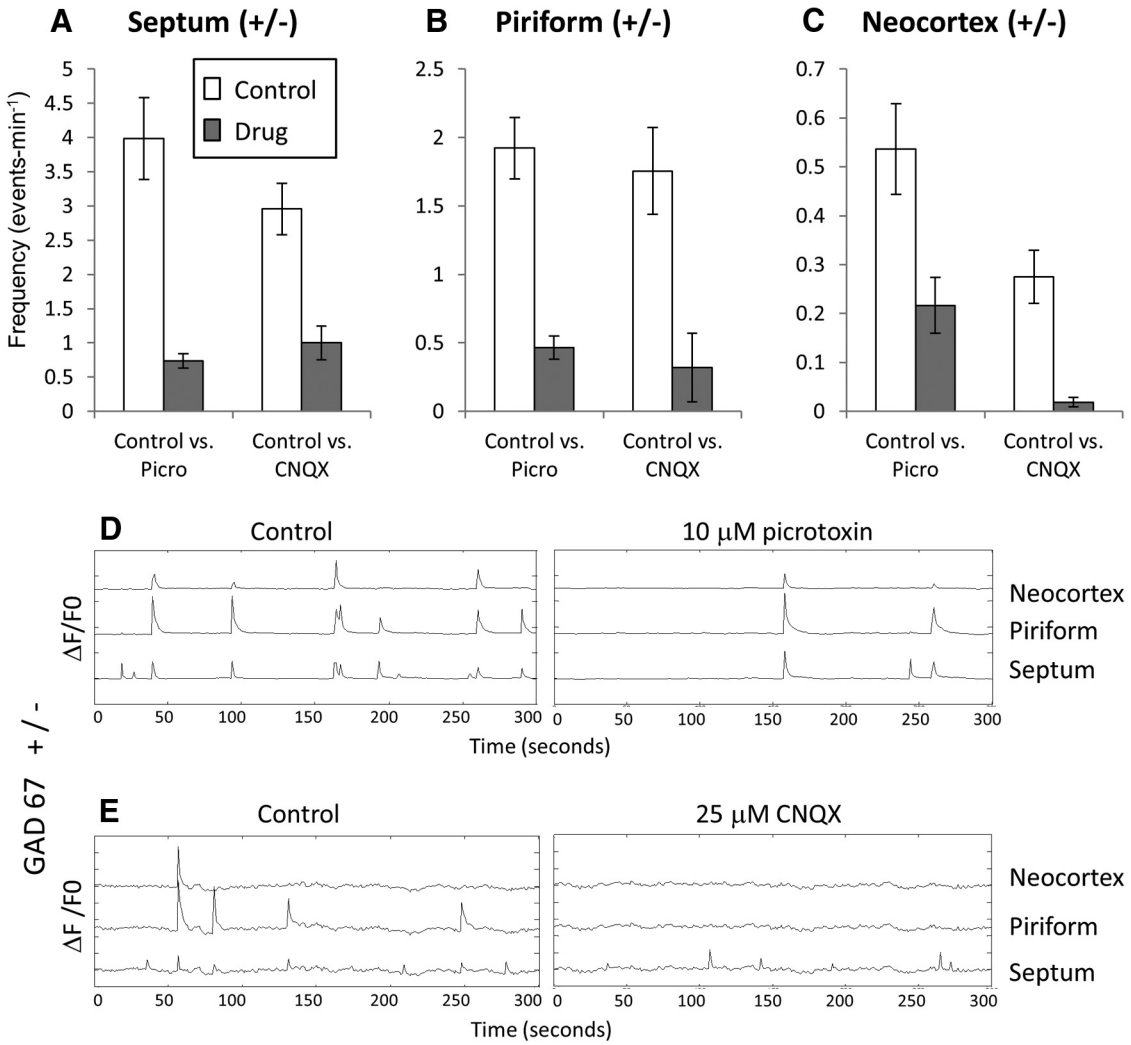

Figure 2. Sensitivity of waves in heterozygote control slices to picrotoxin and CNQX. ***A–C***, Mean wave frequencies in control, picrotoxin, and CNQX measured in the septal nucleus (***A***), piriform cortex (***B***), and neocortex (***C***). Activity in all regions is sensitive to both drugs, but activity in the neocortex is much more sensitive to CNQX than to picrotoxin, suggesting that waves initiated by glutamatergic circuitry are more likely to propagate dorsally than those initiated GABAergically. ***D***, ***E***, Sample fluorescence records in the three regions showing effects of picrotoxin and CNQX. *y*-axis tick marks indicate 10% ΔF/F0.

cordings. Thus, when we refer in this paper to experiments conducted at P0, we reference slices that are E17 + 2 DIV. Our previous work has shown that these cultured slices show normal development of ion channel properties and spontaneous activity compared with acute slices (Picken-Bahrey et al., 2003; McCabe et al., 2006, 2007). In addition, during this period in culture, GFP-labeled interneurons migrate into the dorsal neocortex at approximately the same rate as *in vivo* (unpublished data). Because the *GAD67 KO* mutation used in this study is neonatal lethal (because cleft palate prevents suckling), using cultured slices is the only way we can study the effects of this mutation on spontaneous waves at postnatal stages.

Solutions. ACSF contained (mM) the following: 140 NaCl, 3 KCl, 2 $MgCl_2$, 2 $CaCl_2$, 1.25 $NaHPO_4$, 26.5 $NaHCO_3$, and 20 D-glucose. Picrotoxin and CNQX (Tocris Bioscience) were used at 10 and 25 μM, respectively, in ACSF.

Calcium imaging. Cultured brain slices were removed from the incubator and held in oxygenated ACSF at 28°C for 1–2 h. Slices were then immersed in oxygenated ACSF containing the $[Ca^{2+}]_i$-indicating dye Rhod3 (30 μM) and 0.07% Pluronic F-127 (Invitrogen) for 45–50 min, rinsed, and placed into a glass-bottomed experimental chamber. Rhod3 was used to avoid wavelength overlap with the GFP signal in GABAergic neurons. Oxygenated ACSF (31°C-33°C) was superfused continuously during experiments. Fluorescence images were captured at 1 Hz with either a QuantEM512SC camera (Photometrics) mounted on a Nikon AZ100 microscope, or an OrcaFlash 2.1 camera mounted on an Olympus MVX10 inverted microscope. For experiments where imaging was conducted simultaneously with electrical recordings, an OrcaFlash 2.1 camera was used on an inverted Olympus IX71 inverted microscope. Images were recorded using NIS Elements AR software (Nikon).

Extracellular field potential recordings. Electrical recordings were performed using custom 12-channel, transparent polydimethylsiloxane microfluidic multielectrode arrays (Scott et al., 2013). The microfluidic multielectrode array consists of an array of 12 recording apertures, each 50 μm in diameter, connected to ACSF-filled microfluidic channels leading to Ag/AgCl electrodes that are connected to differential amplifiers (AM Systems; Model 1700). An Ag/AgCl electrode inserted in the bath downstream of the slice serves as a reference electrode. Extracellular electrical signals are digitized (Axon; Digidata 1440) and recorded using pCLAMP 10 software (Molecular Devices) in continuous mode at an acquisition frequency of 10 kHz. In some experiments, we took advantage of the optical transparency of these arrays to perform simultaneous extracellular recording and calcium imaging of wave propagation.

Data analysis. For imaging experiments, Rhod3 fluorescence images of entire brain slices were captured at 1 Hz. Analysis of these image stacks was performed using custom MATLAB (MathWorks) routines. To create summary plots, such as those shown in Figure 2*D*, ROIs were placed

over the septal nucleus, the piriform cortex, and the neocortex and mean (ΔF/F0) signals calculated for each ROI over the entire time course of the image stack. Events were threshold detected at 3 SDs above mean baseline, and frequency of events tabulated for each ROI. To create pseudocolored images of spontaneous waves (see Fig. 1*C*,*D* and Movies 1 and 2), fluorescence images were converted to ΔF/F0 images by subtracting an initial image of Rhod3 fluorescence from each subsequent image in the time series and then dividing each image by the same initial image. The ΔF/F0 record was then thresholded (by zeroing pixel values below a criteria of 3–5% ΔF/F), pseudocolored, and superimposed onto grayscale images of the slice. For each frame, the pixels of the slice image were blanked under the fluorescence signal to preserve the magnitude of the ΔF/F0 signal for the events. These images allowed wave propagation to be correlated with slice anatomy. For electrical experiments, custom MATLAB routines were used to detect and analyze local field potentials (LFPs) and to record their times of occurrence. An 80 Hz lowpass filter was applied to LFP data, and then the signal amplitude was determined by finding the difference between the maximum and minimum signal during the event. The duration of each event was defined as the time over which the amplitude of the signal was >20 times the SD of the noise floor. The power was calculated by integrating the power spectral density of the signal from zero to 80 Hz. Properties of the LFP were first averaged over the five dorsal- or ventral-most recording apertures for each wave, depending on which region was being examined. *N* values reflect the number of such averages that were included in the analysis.

Results

Calcium imaging reveals two forms of activity in coronal slices of mouse forebrain

In previous experiments, we showed, that throughout the period of their occurrence (E18-P8), spontaneous waves of activity in the mouse cortex initiated either in the septal nucleus of the thalamus or in the piriform cortex (Conhaim et al., 2010). From those initiation points, waves either propagated to the rhinal fissure and stopped ("local waves") or crossed the rhinal fissure into the neocortex ("propagating waves") (for locations of these structures in the coronal slices, see Fig. 1*C*). The fraction of propagating waves increased steadily during development, paralleled by an increase in the sensitivity of waves to the glutamate AMPA receptor blocker CNQX, and a decrease in their sensitivity to the $GABA_A$ receptor blocker picrotoxin (Conhaim et al., 2011). These data suggested the hypothesis that local waves at early stages were initiated by a GABAergic pacemaker, whereas propagating waves at later stages were initiated by a glutamatergic pacemaker but did not prove that there were two separate pacemakers. In the present experiments, we eliminated GABAergic transmission genetically by knocking out the major synthetic enzyme for GABA, GAD67, to test the two-pacemaker hypothesis. We used slices from CD1 mice heterozygous for the GAD67 mutation ($GAD67^{+/-}$) as controls because the KO of GAD67 is achieved by GFP knock-in and we wanted to maintain constant imaging conditions between control and experimental groups. Activity was imaged with the calcium indicator dye Rhod 3 to avoid overlap of standard green calcium indicator dyes with GFP expression.

To confirm that spontaneous wave activity was similar in the *CD1* genetic background to that recorded in our previous experiments in Swiss-Webster mice, we measured waves in E17 + 2–3 DIV (P0-P1) $GAD67^{+/-}$ slices by drawing ROIs in three areas: the septum, piriform cortex, and neocortex (Fig. 1*A*, *C*). In the 46 hemispheres that were imaged, waves in heterozygous animals resembled those recorded in previous experiments from Swiss-Webster wild-type animals (Conhaim et al., 2011), with the highest frequencies of activity observed in the septum and piriform cortex (3.37 ± 0.30 and 1.87 ± 0.14 events per minute, respectively; mean ± SEM) and lower frequencies observed in the neocortex (0.39 ± 0.04 events per minute). Examples of waves recorded in the three regions and a montage of local and propagating waves are shown in Figure 1*B–D*.

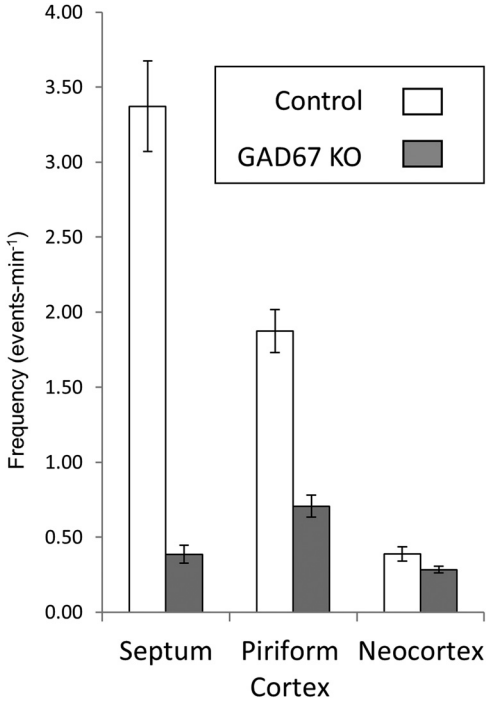

Figure 3. Effects of GAD67 KO on wave frequency and propagation. Wave frequencies in heterozygote control slices and GAD67 KO slices in septum, piriform cortex, and neocortex. The effects of GAD67 KO are similar to the effects of picrotoxin, showing substantial block of activity in septum and piriform cortex, but minimal effect in the neocortex.

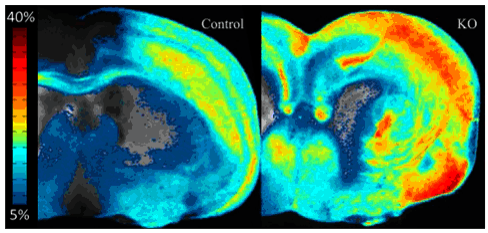

Movie 1. Preferential block of local waves by GAD 67 KO. Films of activity in a heterozygote control and GAD67 KO slice. The control slice shows both local and propagating waves, whereas the KO slice shows only fully propagating waves. Both slices are taken from the same rostral–caudal level. Fluorescence scale is ΔF/F0.

To test for GABA and glutamate involvement in generating wave activity, we applied picrotoxin and CNQX, respectively, to control slices. Both drugs reduced wave frequency substantially in the septum and piriform cortex, the two putative pacemaker regions (Fig. 2*A*,*B*). In agreement with previous results on Swiss-Webster mice, CNQX exerted a much more powerful block of fully propagating waves (96.7 ± 3.3%; $p = 0.001$) than did picrotoxin (64.6 ± 7.6%; $p = 0.01$), as measured by its effect on neocortical activity (Fig. 2*C*). The difference between the block exerted by the two drugs was significant ($p = 0.003$). Figure 2 *D*, *E* shows records of the effects of picrotoxin and CNQX on waves in the septum, piriform cortex, and neocortex. The combination of the two drugs eliminated all waves in all slices. These data indicate that both GABAergic and glutamatergic neurons are involved in initiating spontaneous waves and that glutamatergic

transmission is preferentially involved in propagation of waves into the dorsal neocortex.

Genetic KO of GAD67 eliminates GABAergic waves but spares glutamatergic waves

We next tested the hypothesis that separate GABAergic and glutamatergic pacemaker circuits exist in the septum and piriform cortex, each capable of generating waves. To do this, we compared wave properties in slices from KO mice homozygous for the GAD67 mutation (*GAD67 KO*) to wave properties in control slices ($GAD67^{+/-}$). We predicted that waves in KO slices would show a reduction in the frequency of activity in the septal and piriform regions compared with controls, similar to the reduction seen when control slices were treated with picrotoxin. That is, GAD67 KO should eliminate the picrotoxin-sensitive fraction of waves. Additionally, we predicted that in KO slices the frequency of dorsally propagating waves would be minimally reduced versus controls, given their relatively lesser sensitivity to picrotoxin than to CNQX (Fig. 2*C*).

The data in Figure 3 show that these predictions were correct. Wave frequencies in the septum and piriform regions were reduced in GAD67 KO slices by amounts not significantly different from those observed in control slices when picrotoxin was applied (Fig. 2). Waves in the septum were reduced in the *GAD67 KO* by 88.6 ± 10.6% compared with 81.6 ± 2.0% by picrotoxin ($p = 0.33$, *GAD67 KO* vs picrotoxin). In the piriform region, waves were reduced in the *GAD67 KO* by 62.2 ± 13.2% compared with 79.3 ± 3% by picrotoxin ($p = 0.22$). The frequency of fully propagating waves, as measured in the neocortex, was affected somewhat less by GAD67 KO, with only a 26.9 ± 3.2% reduction in activity versus the 59.6 ± 6.6% reduction seen in picrotoxin experiments ($p = 0.004$). This difference might reflect a contribution of GABA synthetic pathways not dependent on GAD67 in the neocortex at these stages, the block of GABA action on $GABA_B$ receptors by GAD67 KO but not picrotoxin, or actions of picrotoxin not related to $GABA_A$ receptor block. Movie 1 shows waves in control and KO slices, illustrating the preferential sparing of fully propagating waves in KO slices.

These data indicate that two separate wave-initiating circuits exist in the septum and piriform cortex, each of which can initiate waves without the direct participation of the other and that the glutamatergic circuit preferentially initiates waves that propagate across the rhinal fissure into the neocortex.

If this conclusion is correct and GAD67 KO selectively eliminates GABAergic waves, then the waves remaining in the *GAD67 KO* slices should be completely blocked by CNQX and show minimal sensitivity to picrotoxin. The data in Figure 4 show that this is the case. Picrotoxin had no significant effect on wave frequency in the septal and piriform regions ($p = 0.26$ and $p = 0.86$ for septum and piriform data, respectively; $n = 16$ for both), whereas CNQX blocked septal activity by 94.4 ± 3.7%, piriform activity by 97.6 ± 1.8%, and neocortical activity by 95 ± 2.3% (Fig. 4*A–E*; mean ± SEM; $n = 12$ and $p < 0.001$ for all). Picrotoxin did reduce the frequency of fully propagating waves (Fig. 4*C*) somewhat (by 39 ± 9% of control; mean ± SEM, $n = 16$; $p = 0.001$), suggesting that in the neocortex there might be residual GABA signaling via production of GABA from the 65 kDA GAD isoform. Figure 4*D*, *E* shows records of wave activity in the three regions in GAD67 KO slices exposed to picrotoxin and CNQX.

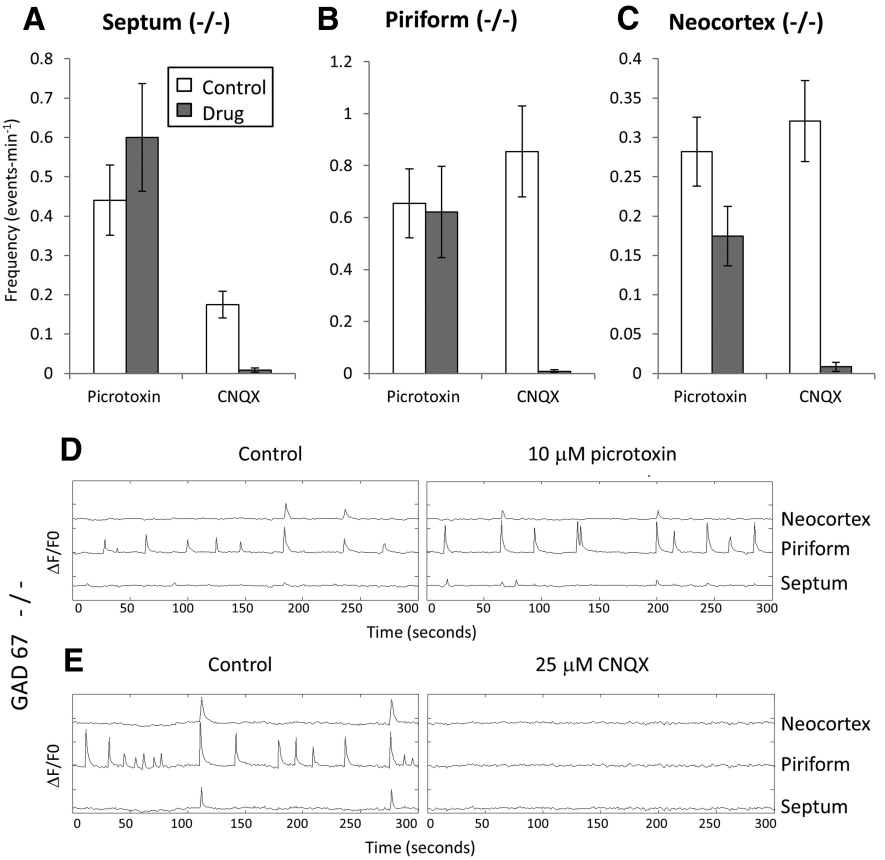

Figure 4. Elimination of picrotoxin sensitivity in GAD67 KO slices. ***A–C***, Mean wave frequencies in control, picrotoxin, and CNQX measured in the septal nucleus (***A***), piriform cortex (***B***), and neocortex (***C***) of GAD67 KO slices. In contrast to control slices (Fig. 2), activity in KO slices shows minimal picrotoxin sensitivity, and is completely blocked by CNQX. The small degree of block of neocortical activity by picrotoxin may reflect a synthetic pathway for GABA in that region that does not depend on GAD67. ***D***, ***E***, Sample records showing lack of picrotoxin sensitivity and block by CNQX of waves in GAD67 KO slices. *y*-axis tick marks are 10% ΔF/F0.

The development of glutamatergic waves does not require GABAergic activity

At the earliest stages of wave occurrence (E17-E18), waves are almost exclusively GABAergic (Conhaim et al., 2011). The fact that the glutamatergic pacemaker appears later but in the same piriform location as the GABAergic activity suggests the hypothesis that the glutamatergic pacemaker develops as a result of preceding GABAergic wave activity. This could occur, for example, if GABA-driven synchronous activity in piriform glutamatergic neurons strengthened synthases within the glutamatergic circuitry using coincidence-detection mechanisms (Kasyanov et al., 2004; Voigt et al., 2005). Chronic elimination of GABAergic waves with GAD67 KO leaves intact a frequency of glutamatergic waves that is similar to what is observed in control slices treated acutely with picrotoxin (compare Figs. 2 and 3), arguing against an absolute dependence of the appearance of the glutamatergic pacemaker on preceding GABAergic waves.

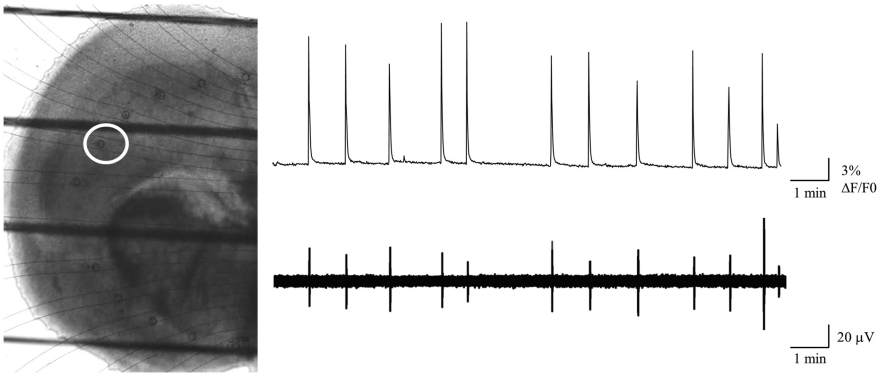

Figure 5. Simultaneous calcium imaging and extracellular array recording of waves using a microfluidic electrode array. Left, Visible light image of an E17 + 2 DIV (P0) coronal slice placed on the microfluidic recording array. The dark horizontal lines indicate the strings of the harp used to stabilize the slice. The faint curved lines indicate the microfluidic channels connecting the recording apertures to the amplifier connections. The white circle surrounds the aperture from which the electrical recordings illustrated were taken, and was used as the ROI for the calcium imaging record. Right, top, Mean Rhod3 fluorescence from the region indicated. Right, bottom, LFPs recorded at the same time as the Rhod3 fluorescence, from the aperture inside the red region. The 1:1 correspondence between electrical and optical measurements of wave activity.

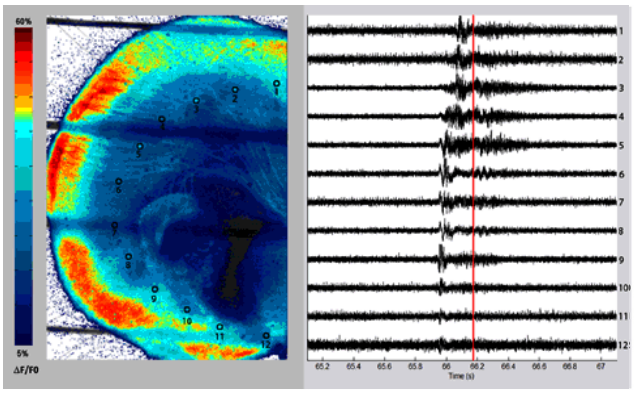

Movie 2. Simultaneous recording of a propagating wave using Ca^{2+} imaging (left) and the microfluidic extracellular array (right). The 12 recording apertures are placed along the path of wave propagation with apertues 8–12 in the piriform initiation region. Aperture positions are indicated by small numbered circles on the slice image and by numbers to the right of the electrical recordings. The Ca^{2+} signal lags behind the electrical recording and lasts longer. The electrical recordings show a clear delay between ventral piriform and dorsal neocortical sites and indicate the speed of wave propagation. In local waves, the field potential signals at the dorsal sites would be absent. Fluorescence scale is ΔF/F0.

These data also indicate that there is little compensatory increase in the output of the glutamatergic pacemaker as a result of the absence of GABAergic waves, as might be predicted from similar homeostatic changes in circuitry mediating other forms of spontaneous activity in the developing CNS (Chub and O'Donovan, 1998). That is, in a developmental context, the two pacemakers appear to operate independently of one another.

Different electrical signatures of the two pacemakers

If there are two semi-independent pacemaker circuits within the piriform cortex, then GABAergic and glutamatergic waves might show different electrophysiological signatures at the site of initiation. To test this hypothesis, we made multisite LFP recordings using a newly developed microfluidic recording array (Scott et al., 2013). This array uses 50 μm fluid-filled recording apertures fabricated into a polydimethylsiloxane substrate, 3D printed onto a glass coverslip, and placed in an arc along the ventral–dorsal path of wave propagation. The apertures are connected via larger fluid-filled channels to remote electrical contacts, resulting in an optically transparent recording array that permits simultaneous calcium imaging to confirm the correspondence of the electrical and calcium signatures of the waves. LFPs show close correlation with calcium waves detected optically (Fig. 5), and the ventral–dorsal propagation direction seen in imaging experiments is reflected in the progressive delay in the field potential onset at more dorsal recording apertures (Movie 2). Movie 2 illustrates simultaneous electrical and optical recording of waves from a coronal slice using this array.

To test the hypothesis that GABAergic and glutamatergic pacemakers could be distinguished by their electrical signals at the site of wave initiation, we recorded 218 local and 132 propagating waves from seven control slices and sorted the LFPs at the ventral, piriform wave initiation site into those that initiated local versus propagating waves. Analysis of these signals showed that, on average, LFPs at the site of wave initiation were longer in duration and larger in amplitude for propagating waves than for local waves (duration: 343 ± 17 ms vs 170 ± 9.7 ms; p = 6.13E-17; amplitude: 32.78 ± 1.76 μV vs 13.70 ± 0.79 μV, p = 9E-19) (Fig. 6*A–C*). A scatter plot of LFP duration versus amplitude for all slices (Fig. 6*D*) shows that, even with between-slice variability in overall event amplitudes and durations, local versus propagating waves can be distinguished with reasonable accuracy from the properties of their field potentials at the point of origin in the piriform cortex. For example, for the data in Figure 6*D*, 70% of LFPs (red symbols) were <8 μV in amplitude or <0.15 s in duration, whereas 87% of propagating wave LFPs fell outside of these ranges (dashed lines). Within single slices, the accuracy in predicting whether a wave propagates or not based on piriform LFP amplitude and duration was even higher. For the slice shown in Figure 6*E*, a simple amplitude criterion of 51 μV predicted 100% of propagating waves (red symbols) and 94% of local waves. These results are consistent with the idea that two different initiation circuits exist within the pacemaker region for local and propagating waves and that the glutamatergic network in the piriform cortex must be recruited into waves in order for them to propagate into the neocortex.

Interactions between GABAergic and glutamatergic initiation circuits

We next asked whether the GABAergic and glutamatergic circuits involved in wave initiation interacted with each other during wave propagation. The ability of GABA at these stages to initiate wave events ventrally indicates that GABA is excitatory, in the sense that V_{Cl} is positive to threshold and GABA can excite quiescent neurons (Owens et al., 1996). However the shunting effect of $GABA_A$ channels and the fact that V_{GABA} is negative to $V_{Glutamate}$ raise the possibility that GABAergic action might also inhibit glutamatergic waves.

First, we asked whether dorsal LFPs during glutamatergic waves were different in control and *GAD67 KO* slices. GAD67 KO increased the peak amplitude of the dorsally recorded LFP during glutamatergic waves (control: 32.32 ± 1.83 μV, n = 136 waves in 5 slices; KO: 41.4 ± 1.1 μV, n = 220 waves in 5 slices; p = 0.038) (Fig. 7*A*). GAD67 KO also caused the appearance of a pronounced 35 Hz oscillation at the end of the LFP, seen as a modest

increase in signal duration (control: 510 ± 16 ms; KO: 553 ± 12 ms; p = 2.65E-05; same n values as amplitude) and a large increase the total power of the signal (control: 3.67 ± 0.32 μV^2; KO: 6.72 ± 0.42 μV^2; p = 2.15E-08) (Fig. 7*B–D*). Exposure of control slices to picrotoxin also caused the appearance of an ~35 Hz oscillation in the latter phase of the LFP (Fig. 7*D*), which resulted in a significant increase in total power (7.57 ± 1.15 μV^2, n = 186 waves in 4 slices; p = 0.001 vs control, 0.49 vs KO) (Fig. 7*C*). The changes in amplitude and duration of the LFP caused by picrotoxin appeared to be in the same direction as those caused by GAD67 KO but were not statistically significant. The increase in power is the result of the introduction of the 35 Hz oscillation onto the later half of the LFP, which causes the LFP to approach its maximum amplitude for a greater proportion of its duration, rather than having a single spike at the beginning of the LFP that sets peak amplitude, as seen in control traces. These data suggest that GABAergic transmission inhibits glutamatergic waves in the neocortex, possibly by a combination of reducing the number of neurons participating in the waves and reducing the number of action potentials generated by each neuron during a wave.

We next asked whether the initiation of glutamatergic waves in the piriform pacemaker was affected by the absence of GABAergic transmission. We showed above a close correspondence between LFPs recorded with our microfluidic array and waves recorded by calcium imaging. In *GAD67 KO* slices, however, the electrical burst structure underlying wave initiation in the piriform cortex is more complex than in controls. In KO slices, an LFP recorded in the piriform initiator region would often be followed very closely by other LFPs (Fig. 8*A*), with event intervals that were sometimes faster than the 1 Hz acquisition rate used for calcium imaging experiments. Thus, in the KO, a single event recorded with calcium imaging techniques might actually be composed of multiple electrical field potentials. In a few cases where electrical and imaging recordings were conducted simultaneously and images were acquired at 2 Hz, closely spaced LFPs were picked up in the calcium imaging record as a calcium transient with multiple peaks (data not shown). The same effect was seen in control slices exposed to picrotoxin (data not shown). To confirm increased tendency of field potentials underlying waves in the *GAD67 KO* slices to burst, we constructed

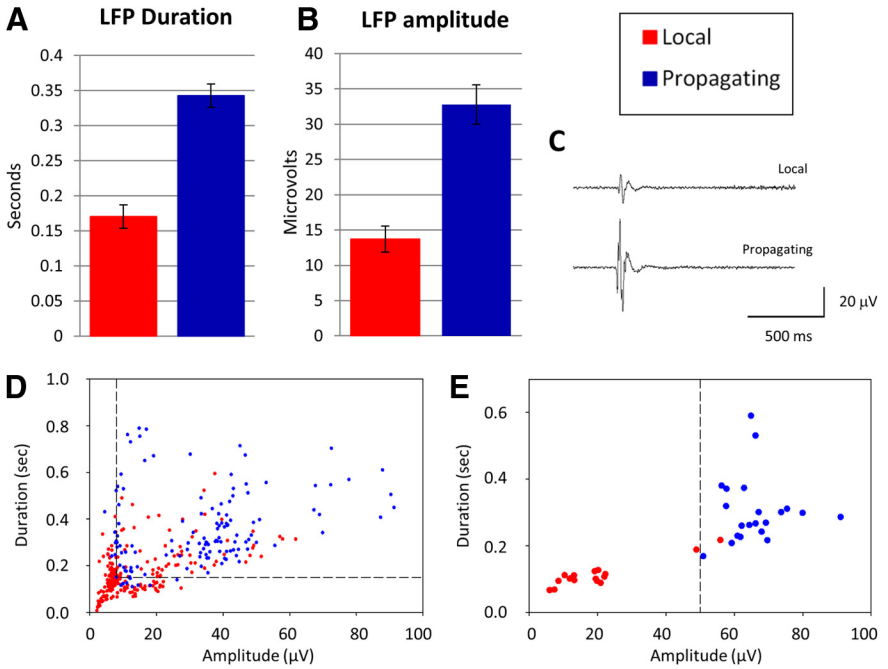

Figure 6. Local and propagating waves can be distinguished by their LFPs at the site of initiation in the piriform cortex. ***A***, ***B***, LFPs in the piriform cortex are larger in amplitude and longer in duration for waves that propagate into the dorsal neocortex. ***C***, Examples of LFPs for local and propagating waves. ***D***, Scatter plot of LFP duration versus amplitude for all slices show clustering of LFPs for local versus propagating waves. Dashed lines indicate criterion values giving maximal separation of the waveforms (see Results). ***E***, In individual slices, where there is less variation in overall mean LFP amplitude, clustering of local and propagating wave LFPs is more prominent. Dashed line indicates amplitude criterion that separates 100% of propagating wave LFPs and 94% of local wave LFPs (see Results).

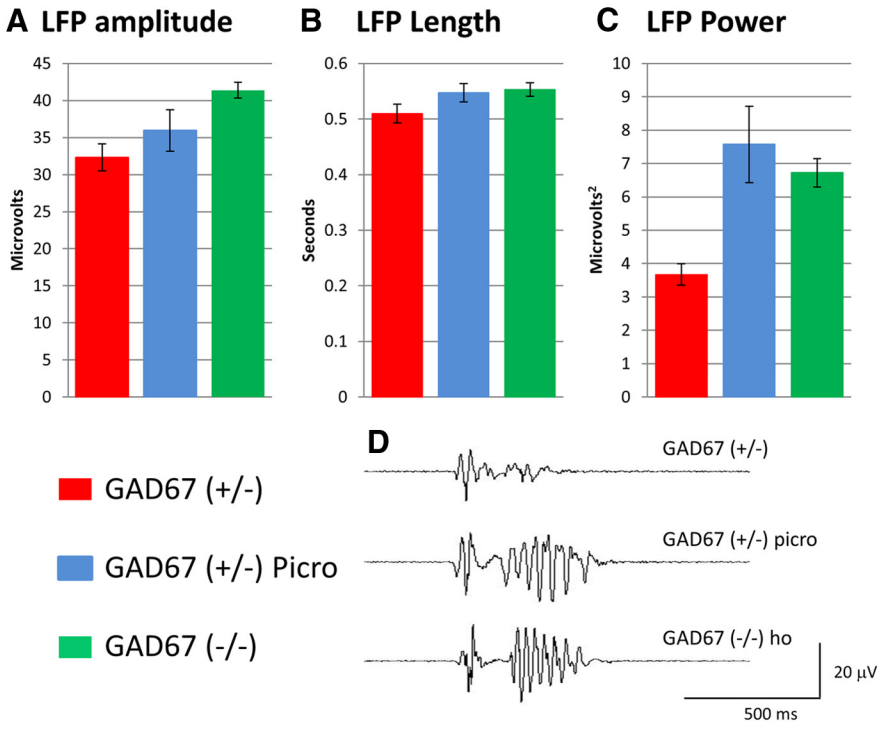

Figure 7. Blocking GABA enhances the power of the LFP during neocortical glutamatergic waves. ***A–C***, GAD67 KO increases the amplitude, duration, and total power of neocortical LFPs. Application of picrotoxin to control slices has similar, though not significant, effects on field potential amplitude and duration, and increases field potential power by the same amount as GAD67 KO (***C***). ***D***, Sample records of dorsal LFPs in control, GAD67 KO, and control + picrotoxin slices showing late 35 Hz oscillation induced by GAD67 KO or picrotoxin. This indicates that GABA inhibits glutamatergic waves dorsally in the neocortex.

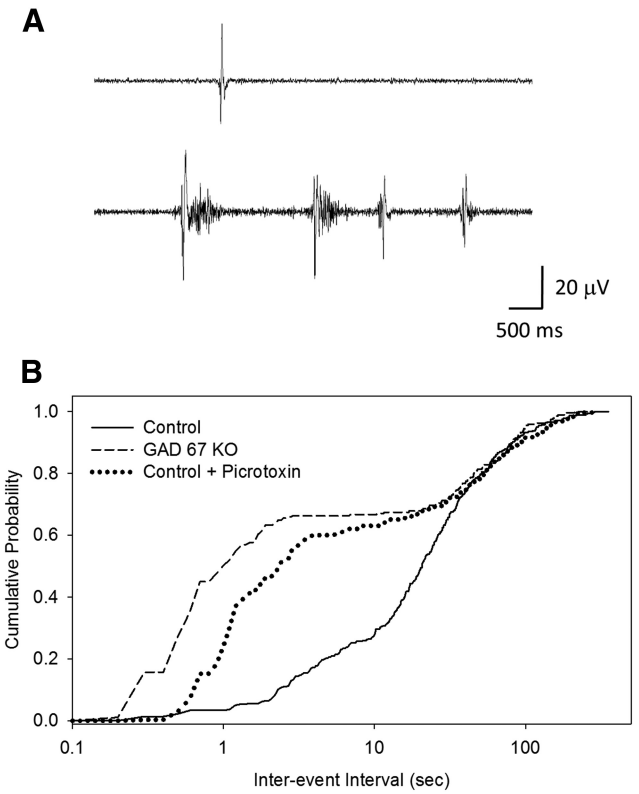

Figure 8. Interaction between GABAergic and glutamatergic pacemakers in the piriform cortex. ***A***, GAD67 KO induces bursting of LFPs in the piriform cortex underlying single glutamatergic waves. LFP recordings corresponding to single waves are shown for control (top) and GAD67 KO slices (bottom). ***B***, Cumulative probability plots of LFP intervals in control, GAD67 KO, and control + picrotoxin slices. Control slices show a single distribution of interevent intervals, whereas both GAD67 KO and picrotoxin slices show the appearance of a second, short-interval population corresponding to rapid bursts of events that give rise to single waves as detected by calcium imaging.

cumulative probability plots of the intervals between LFPs for the piriform region in control, GAD67 KO, and control + picrotoxin slices (Fig. 8*B*). In control slices, this plot shows a single sigmoidal distribution with a mean interval reflecting the mean wave frequency of ~2 events per minute recorded in imaging experiments (Fig. 3). In contrast, LFP intervals in the *GAD67 KO* slices showed a bimodal distribution reflecting the addition of a second population of short intervals corresponding to high-frequency bursts. For example, in the *GAD67 KO* slices, ~50% of intervals were less than the 1 s interval used for image acquisition in calcium imaging experiments, whereas in control slices <2% fell into this category. Treatment of control slices with picrotoxin produced a similar change in the cumulative probability plots (Fig. 8*B*). These results indicate that, in the absence of GABAergic transmission, the glutamatergic pacemaker is more active electrically and operates in bursts of activity rather than single events.

Thus, GABAergic neurons in both piriform and neocortical regions exert an inhibitory influence on the glutamatergic wave activity. This raises an interesting paradox because the GABAergic pacemaker initiates waves at these stages, indicating that GABAergic transmission is excitatory. One possibility to explain these data is that GABAergic waves reflect excitation only within the GABAergic neuronal population, whereas GABAergic inputs to glutamatergic neurons might be inhibitory, reflecting a lower intracellular chloride concentration in the glutamatergic neurons. We tested whether the GABAergic pacemaker could excite glutamatergic neurons by asking whether glutamatergic neurons are recruited into waves initiated GABAergically. To do this, we measured calcium transient amplitudes in the piriform cortex during waves before and after treatment with CNQX under conditions where CNQX had no effect on wave frequency (i.e., where wave initiation was driven entirely by the GABAergic pacemaker). Under these conditions, CNQX caused a substantial reduction in the amplitude of calcium transients (from 9.57 ± 2.59 to 5.73 ± 1.54% ΔF/F0, $p = 0.017$), indicating that the GABAergic pacemaker that initiated the waves recruited glutamatergic neurons to participate in the waves. Thus, at stages when GABAergic neurons initiate waves and excite glutamatergic neurons, they also inhibit glutamatergic network activity. Possible mechanisms underlying this apparently dual action of the GABAergic pacemaker circuit are discussed below.

Discussion

Waves of spontaneous electrical activity propagate across the mouse cerebral cortex early in development. These waves are initiated in the septum or piriform cortex and may or may not propagate across the rhinal fissure to invade the neocortex. Waves are sensitive to blockers of $GABA_A$ and AMPA receptors, indicating that both transmitters are involved in wave initiation (Conhaim et al., 2011). It was not clear, however, from past experiments whether one pacemaker circuit exists with a neurotransmitter dependency that changes from GABAergic to glutamatergic, or whether there are two separate pacemaker circuits, each individually capable of wave initiation, that are expressed sequentially in development. In this paper, we used genetic elimination of GAD67, the primary enzyme for GABA synthesis at these stages, to test the hypothesis that there are two semi-independent pacemakers that initiate these waves: one GABAergic and the other glutamatergic.

In slices from *GAD67 KO* cortex, wave frequency was reduced by an amount predicted from the picrotoxin-sensitive fraction of waves in control slices, and wave sensitivity to picrotoxin was eliminated. These data argue that there are two separate pacemakers driving cortical waves. Waves in *GAD67 KO* slices also showed a much stronger tendency to propagate dorsally into the neocortex, confirming our previous conclusion (Conhaim et al., 2011) that the GABAergic pacemaker preferentially triggers waves that remain localized to the piriform cortex, whereas the glutamatergic pacemaker preferentially triggers fully propagating waves.

Our model of wave-initiating circuits in the piriform cortex and their interactions with follower neurons in both the piriform cortex and neocortex is shown in Figure 9. The top row represents generation of a GABAergic wave in a control slice. The GABA pacemaker fires (Frame 1: yellow triangle; asterisk). This recruits both GABAergic and glutamatergic follower cells in the piriform cortex (Frame 2: open triangle and circle). Because these waves rarely propagate across the rhinal fissure, we propose that the neurons recruited by the GABAergic pacemaker do not excite glutamatergic circuitry that spans the rhinal fissure (yellow ellipse). This wave propagates to the rhinal fissure (Frame 3) but does not cross it (Frame 4). The second row shows generation of a glutamatergic wave in a control slice. The glutamatergic pacemaker fires (yellow circle; asterisk) but, because it is normally inhibited by GABAergic neurons in the piriform cortex (yellow open triangle, red bar), it fires only a single LFP (inset, Frame 1). This recruits glutamatergic circuitry both locally in the piriform cortex (yellow circle) (Frame 2) and at the rhinal fissure (yellow ellipse), allowing these waves to reach the rhinal fissure (Frame 3)

and cross into the neocortex (Frame 4). In the neocortex, glutamatergic circuitry is inhibited by GABAergic neurons, giving rise to an LFP without pronounced after-oscillations (inset, Frame 4). The third row represents generation of glutamatergic waves in *GAD67 KO* slices. The glutamatergic pacemaker in the piriform cortex fires, but, because it is not inhibited by local GABAergic neurons, it fires a burst of LPFs (inset, Frame 1). This recruits glutamatergic circuitry as in the control, and the wave propagates into the neocortex. In the neocortex, GABA inhibition is not present, so glutamatergic activity shows pronounced after-oscillations in the LFP (inset, Frame 4). GABAergic inhibition in this model occurs only when target cells are active, as discussed above.

Do symptoms of the *GAD67 KO* mouse suggest a developmental function for GABAergic waves? The *GAD67 KO* mouse dies at P0. Although Asada et al. (1997) reported that this mouse has normal gross cortical anatomy, they by necessity examined brains only up to P0. Any abnormalities resulting from the absence of GABAergic waves would be expected to appear only later in development, after the period during which these waves occur. It may be possible in future experiments to examine such abnormalities in cultured slices, which can be prepared before P0 and held in culture until later chronological stages.

Our previous data showed that the picrotoxin sensitivity of waves decreased over developmental time, presumably reflecting the fact that GABA becomes progressively less excitatory during the first postnatal week of development. Combined with the present data, this indicates a model in which the GABAergic pacemaker becomes progressively less important over developmental time, whereas the glutamatergic pacemaker assumes the dominant role in wave initiation. The complexity of wave initiation mechanisms presumably reflects the dynamic nature of cortical circuitry during a period of development when both GABAergic interneurons and glutamatergic pyramidal neurons are migrating, and when the changing levels of expression of chloride transporters gives rise to continuous changes in the strength and sign of GABAergic synaptic inputs to both GABAergic and glutamatergic neurons. This all occurs even as activity-dependent developmental programs continue to require spontaneous activity.

Our results differ from the pattern reported by Allène et al. (2008), who found that early synchronous activity was more dependent on glutamatergic transmission and only later transitioned to being GABA-dependent. This result is somewhat counterintuitive, given the fact that GABA is more excitatory at earlier stages of development (see, e.g., Owens et al., 1996). Allène et al. (2008) worked primarily in horizontal slices, which are likely not to include the piriform cortex where our GABAergic pacemaker resides. Thus, they may have excluded GABAergic waves in many of their experiments. In addition, when using relatively small imaging regions, it can be difficult to determine whether local synchrony results from the passage of a propagating wave through the field or some other form of correlated activity. We do not think that our early GABAergic waves result from using cultured slices because the stages at which GABAergic waves are most prominent are those at which the slices have been in culture the shortest period of time. We agree with Allène et al. (2008), however, that there are likely to be multiple forms of correlated activity in the developing brain, all represented to some extent throughout this critical period of development. For example, Yang et al. (2009, 2013) reported activity at these stages that depends on thalamic and/or peripheral inputs to the cortex. We have recorded local correlated activity between E18 and P4 that depends on gap junctional communication (S. C. Barnett, unpublished data), as well as wave activity that arises in various subcortical structures (Z. Barger, unpublished data).

Our data also indicate that GABAergic neurons as a population can simultaneously act to trigger waves, recruit glutamatergic neurons into those waves, and inhibit glutamatergic network activity. At the stages we are examining in heterozygous slices, between 65% and 80% of waves are initiated by GABAergic neurons. Glutamatergic neurons are recruited into these waves, as indicated by the decrease in calcium transient amplitude in the

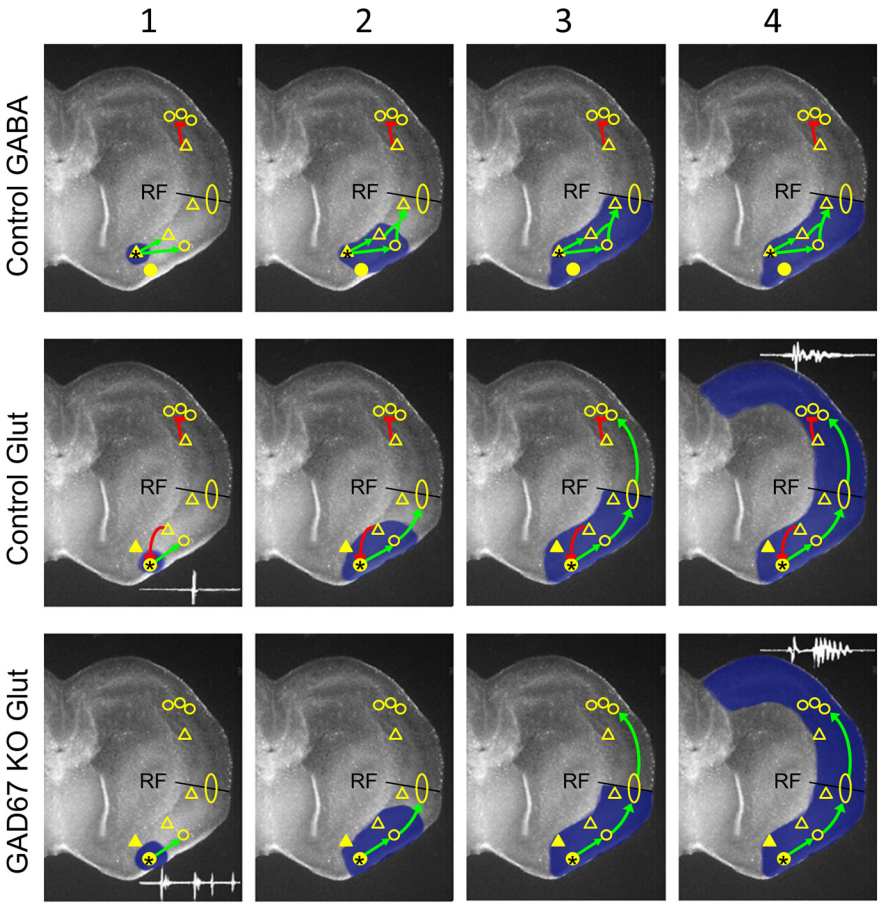

Figure 9. Circuit model of wave initiation and propagation (see text for full description of model). Yellow circles represent glutamatergic circuitry. Triangles represent GABAergic circuitry. Filled symbols represent initiators. Open symbols represent followers. The yellow ellipse indicates proposed glutamatergic circuitry that spans the rhinal fissure and triggers neocortical waves. RF, Rhinal fissure separating the piriform cortex (below) from the neocortex (above). Green arrows indicate excitation. Red bar lines indicate inhibition. The sequence of initiation and propagation is depicted for GABAergic waves in control slices (top row), glutamatergic waves in control slices (middle row), and glutamatergic waves in GAD67 KO slices (bottom row). Sequence of events proceeds left to right in columns 1–4.

piriform cortex during the waves by CNQX. The glutamatergic waves are inhibited by GABAergic neurons, as indicated by the effect of the GAD67 KO on LFP waveform in the neocortex, and by the increase in LFP bursts associated with waves in the GAD67 KO. How can GABA be simultaneously excitatory and inhibitory to the glutamatergic circuitry? One possibility is that the population of glutamatergic neurons is not uniform. Less mature neurons, presumably with higher levels of intracellular chloride, might be the population that is recruited into waves by the GABAergic pacemaker because GABA is more excitatory to those cells. More mature neurons, with lower intracellular chloride levels, might form the core of the network generating oscillations in the neocortex and be more inhibited by GABAergic inputs. But there are other possible explanations. Even at stages when GABA is most excitatory, measured GABA reversal potentials, although positive to threshold, are still negative to the AMPA receptor reversal potential (Owens et al., 1996). In this situation, GABA would be excitatory to quiescent cells but inhibitory to events driven by glutamatergic inputs. Independent of reversal potential considerations, the shunting caused by opening of $GABA_A$ chloride channels would also decrease glutamatergic excitation, not only by reducing input resistance, but also by reducing length and time constants. Thus, defining whether the output of GABAergic circuitry in the piriform cortex is excitatory or inhibitory depends on knowing the state of activity of glutamatergic circuits at that instant in time. When the glutamatergic pacemaker is operating at low frequency, the dominant effect of GABA action on glutamatergic neurons will be excitatory, recruiting them into waves. When the glutamatergic pacemaker is operating at higher frequencies, GABA will tend to inhibit those neurons, reducing the participation of glutamatergic neurons in wave activity. Frequency-dependent transient changes in intracellular chloride concentration may also contribute to these effects. Eventually, by approximately P10, GABA becomes inhibitory in all contexts, and this transition terminates waves entirely, allowing asynchronous circuit activity to emerge in the cortex.

References

Allène C, Cattani A, Ackman JB, Bonifazi P, Aniksztejn L, Ben-Ari Y, Cossart R (2008) Sequential generation of two distinct synapse-driven network patterns in developing neocortex. J Neurosci 28:12851–12863. CrossRef Medline

Asada H, Kawamura Y, Maruyama K, Kume H, Ding RG, Kanbara N, Kuzume H, Sanbo M, Yagi T, Obata K (1997) Cleft palate and decreased brain gamma-aminobutyric acid in mice lacking the 67-kDa isoform of glutamic acid decarboxylase. Proc Natl Acad Sci U S A 94:6496–6499. CrossRef Medline

Blankenship AG, Feller MB (2010) Mechanisms underlying spontaneous patterned activity in developing neural circuits. Nat Rev Neurosci 11:18–29. CrossRef Medline

Chub N, O'Donovan MJ (1998) Blockade and recovery of spontaneous rhythmic activity after application of neurotransmitter antagonists to spinal networks of the chick embryo. J Neurosci 18:294–306. Medline

Conhaim J, Cedarbaum ER, Barahimi M, Moore JG, Becker MI, Gleiss H, Kohl C, Moody WJ (2010) Bimodal septal and cortical triggering and complex propagation patterns of spontaneous waves of activity in the developing mouse cerebral cortex. Dev Neurobiol 70:679–692. CrossRef Medline

Conhaim J, Easton CR, Cedarbaum ER, Barahimi M, Moore JG, Becker MI, Mather LF, Minter DJ, Moen SP, Dabagh S, Moody WJ (2011) Developmental changes in propagation mouse cerebral cortex. J Physiol 589:2529–2541. CrossRef Medline

Corlew R, Bosma MM, Moody WJ (2004) Spontaneous, synchronous electrical activity in neonatal mouse cortical neurons. J Physiol 560:377–390. CrossRef Medline

Garaschuk O, Linn J, Eilers J, Konnerth A (2000) Large-scale oscillatory calcium waves in the immature cortex. Nat Neurosci 3:452–459. CrossRef Medline

Hunt PN, Gust J, McCabe AK, Bosma MM (2006) Primary role of the serotonergic midline system in synchronized spontaneous activity during development of the embryonic mouse hindbrain. J Neurobiol 66:1239–1252. CrossRef Medline

Kasyanov AM, Safiulina VF, Voronin LL, Cherubini E (2004) GABA-mediated giant depolarizing potentials as coincidence detectors for enhancing synaptic efficacy in the developing hippocampus. Proc Natl Acad Sci U S A 101:5311–5312. CrossRef Medline

Lischalk JW, Easton CR, Moody WJ (2009) Bilaterally propagating waves of spontaneous activity arising from discrete pacemakers in the neonatal mouse cerebral cortex. Dev Neurobiol 69:407–414. CrossRef Medline

McCabe AK, Chisholm SL, Picken-Bahrey HL, Moody WJ (2006) The self-regulating nature of spontaneous synchronized activity in developing mouse cortical neurones. J Physiol 577:155–167. CrossRef Medline

McCabe AK, Easton CR, Lischalk JW, Moody WJ (2007) Roles of glutamate and GABA receptors in setting the developmental timing of spontaneous synchronized activity in the developing mouse cortex. Dev Neurobiol 67:1574–1588. CrossRef Medline

Moody WJ Bosma MM (2005) Ion channel development, spontaneous activity, and activity-dependent development in nerve and muscle cells. Physiol Rev 85:883–941. CrossRef Medline

Owens DF, Boyce LH, Davis MB, Kriegstein AR (1996) Excitatory GABA responses in embryonic and neonatal cortical slices demonstrated by gramicidin perforated-patch recordings and calcium imaging. J Neurosci 16:6414–6423. Medline

Picken-Bahrey HL, Albrieux M, Moody WJ (2003) Early development of voltage-gated ion currents and firing properties in neurons of the mouse cerebral cortex. J Neurophysiol 89:1761–1773. Medline

Schneiderman JH (1986) Low concentrations of penicillin reveal rhythmic, synchronous synaptic potentials in hippocampal slice. Brain Res 398:231–241. CrossRef Medline

Scott A, Weir K, Easton C, Huynh W, Moody WJ, Folch A (2013) A microfluidic microelectrode array for simultaneous electrophysiology, chemical stimulation, and imaging of brain slices. Lab Chip 13:527–535. CrossRef Medline

Tamamaki N, Yanagawa Y, Tomioka R, Miyazaki J, Obata K, Kaneko T (2003) Green fluorescent protein expression and colocalization with calretinin, parvalbumin, and somatostatin in the GAD67-GFP knock-in mouse. J Comp Neurol 467:60–79. CrossRef Medline

Voigt T, Opitz T, de Lima AD (2005) Activation of early silent synapses by spontaneous synchronous network activity limits the range of neocortical connections. J Neurosci 25:4605–4615. CrossRef Medline

Wong WT, Myhr KL, Miller ED, Wong RO (2000) Developmental changes in the neurotransmitter regulation of correlated spontaneous retinal activity. J Neurosci 20:351–360. Medline

Yang JW, Hanganu-Opatz IL, Sun JJ, Luhmann HJ (2009) Three patterns of oscillatory activity differentially synchronize developing neocortical networks in vivo. J Neurosci 29:9011–9025. CrossRef Medline

Yang JW, An S, Sun JJ, Reyes-Puerta V, Kindler J, Berger T, Kilb W, Luhmann HJ (2013) Thalamic network oscillations synchronize ontogenetic columns in the newborn rat barrel cortex. Cereb Cortex 23:1299–1316. CrossRef Medline

Zheng J, Lee S, Zhou ZJ (2006) A transient network of intrinsically bursting starburst cells underlies the generation of retinal waves. Nat Neurosci 9:363–371. CrossRef Medline

Chapter Three

Inhibitory interneurons exhibit both L-type calcium channel mediated, asynchronous calcium signals and TTX dependent population activity in developing Tbr1 deficient and wildtype neocortex

Inhibitory interneurons exhibit both L-type calcium channel mediated, asynchronous calcium signals and TTX dependent population activity in developing Tbr1 deficient and wildtype neocortex

Abstract

Cortical development involves initial structuring of network features genetically programmed signaling pathways. Later, ion channel activity helps refine neuronal connections. In this study we examine propagating waves of activity in a mouse genetically engineered to lack the transcription factor T-box, brain 1 (Tbr1), which is involved in the differentiation of cortical excitatory neurons and cortical patterning. Using calcium imaging, we find that despite gross malformations of the cortex associated with this mutation, wave activity appears at normal frequencies. Additionally we examine the distribution of cortical inhibitory neurons in Tbr1 deficient cortex using genetically encoded red-fluorescent-protein (RFP), and find that these neurons are displaced in a manner similar to what is observed in reeler mice. Sensitivity of waves to blockade of GABA signaling is preserved in Tbr1 deficient mice. Finally, we show using dual green and red-channel fluorescence imaging of calcium indicator dye and RFP fluorescence, respectively, that inhibitory interneurons participate in spontaneous calcium events at normal frequencies in Tbr1 deficient mice. We identify two distinct types of spontaneous calcium signals in both wild-type and Tbr1 deficient mice: one that is consistent with wave activity, and another that is restricted to single cells and not correlated with neighboring cells, and sensitive to blockers of L-type calcium channels. These results provide evidence that wave activity is a robust property of developing networks, and establish new methods of recording calcium signals from genetically labeled cell populations. We identify distinct calcium signals in immature interneurons that may serve separate purposes in development.

Introduction

Electrical activity plays important roles in diverse developmental processes from neurogenesis to cell differentiation. The specific properties of the activity regulates distinct developmental functions. Waves of propagating activity occur in the first postnatal week of murine cortex, which consist of burst of action potentials occurring synchronously in a majority of cells of the cortical plate, and are correlated with intracellular calcium oscillations that may be detected with calcium imaging techniques. The proposed roles of waves in cortical development include affecting the migration of inhibitory interneurons to aid in their placement into the correct cortical layers (Bortone et. al. 2009, de Lima et. al. 2009). In this study we examine wave activity in mice expressing genetic deletion of Tbr1, a cortical patterning gene that affects the differentiation of excitatory glutamatergic neurons, which are critical to generating and shaping waves. (Hevner et. al. 2001 and 2002) In addition to reducing the number of glutamatergic neurons in the cortex and the connections these cells make within and outside of the cortex, Tbr1 KO causes aberrant cortical layering. The normal distribution of excitatory cells, an "inside out" organization wherein the first born neurons reside in deeper cortex near the ventricle and younger cells reside in more superficial layers, does not occur without Tbr1. We hypothesized that the effects of Tbr1 KO on glutamatergic cells, as well as the disruption of their layer organization and connectivities, would prevent the normal occurrence of waves.

Our results, however, indicate that this hypothesis was not true, and in fact waves continue in the Tbr1 KO at frequencies comparable to normal conditions. Given this result we conducted pharmacological experiments and hypothesized that waves are able to persist in the Tbr1 KO due to some shift in neurotransmitter dependency that makes up for a loss of glutamatergic signaling, perhaps by an enhanced role of excitatory GABA, which has been shown to play an important role in wave generation. (Conhaim et, al. 2011, Easton et. al. 2014) Additionally we provide a novel study of the morphology of cortical inhibitory interneurons in the Tbr1KO, and show that disorganization of interneurons with the mutation is similar to that observed in reeler mice (Hevner et. al. 2004), which lack the molecule "reelin" that is critical for cortical layer organization.

Finally, we examined calcium transients on a cellular level in WT and Tbr1KO cortex. We find, at similar frequencies in both WT and KO cortex, wave-like activity in individual cells that is synchronous across many cells in the field of view, and also a single-cell, asynchronous calcium signal that does not propagate to other cells. We find that the synchronous signal is selectively blocked by blockers of sodium channels, while the asynchronous signal is more sensitive to blockade of L-type calcium channels. We determined that the two forms of activity are distinct and negatively correlated with each other, such that a cell participating in synchronous activity is less likely to express the asynchronous calcium signal. The negative correlation between these two types of activity could be important, for example, if the two forms of activity regulate a transition between distinct developmental events.

Materials and Methods

Animal procedures – Time-mated females carrying E18 fetuses were killed with carbon dioxide, and the fetuses were removed and placed on ice. Brains were removed from the fetuses and sliced 300μM thick in ice-cold ACSF using a Leica VT1200S vibrating microtome. All animal procedures were approved by the Institutional Animal Care and Use Committee at the University of Washington.

Generation of transgenic animals – Tbr1KO pups were obtained by time mating heterozygous parents, (Tbr1 mouse reference) and identifying pups with reduced olfactory bulb size, the genotype of which were

confirmed with gel PCR. For some experiments, we used a GAD67-GFP knock-in line (Tamamaki et al., 2003) to label interneurons. Control animals were heterozygous for GAD67 GFP and identified by GFP expression. Only one Tbr1KO-GAD67GFP animal was obtained by mating parents heterozygous for both GAD67 GFP and Tbr1, because these genes are located on the same chromosome, making coexpression of Tbr1 and GAD67 impossible without rare recombination events. The single animal obtained through recombination was used as the example in Figure 2 due to the high signal to noise ratio in this set of images.

The rest of the experiments labeling interneurons utilized a red-fluorescent-protein (RFP) label. RFP expression was achieved by pairing the Cre-dependent Ai14 mouse, which expresses tdtomato under control of the Rosa26 promoter, with a mouse expressing Cre under control of the Dlx5/6 promoter (Jackson labs). For wild-type experiments, homozygous or heterozygous Dlx-Cre males were time mated with homozygous Ai14 females. For Tbr1 experiments, males were heterozygous for Dlx-Cre and heterozygous for Tbr1KO, while females were homozygous for Ai14 and heterozygous for Tbr1KO. This arrangement allowed for all Tbr1KO animals to have RFP labeled interneurons.

Slice cultures – Coronal slices were taken from fetuses at a position anterior to the hippocampus and posterior to the olfactory bulbs, where the lateral ventricles were clearly visible. Slices were cultured as described in Easton et. al. 2014 with some changes to the time and duration of culture. Tbr1KO animals were sliced at E17 and cultured for 2-9 days, whereas RFP labeled slices were taken at E18, due to the smaller size of pups from the C57 Bl/6 background of the mothers. RFP positive slices were cultured for 2–3 d and then removed from the incubator and placed into ACSF for physiological recordings. Thus, when we refer in this paper to experiments conducted at P2, we reference slices that are E17 + 3 DIV for Tbr1 KO slices, or E18 + 2DIV for RFP labeled slices. Our previous work has shown that these cultured slices show normal development of ion channel properties and spontaneous activity compared with acute slices (Picken-Bahrey et al., 2003; McCabe et al., 2006, 2007). In addition, during this period in culture, GFP-labeled interneurons migrate into the dorsal neocortex at approximately the same rate as in vivo (unpublished data). Because the Tbr1 KO mutation used in this study is neonate-lethal, using cultured slices is the only way we can study the effects of this mutation on spontaneous waves at postnatal stages.

Solutions – ACSF contained (mM) the following: 140 NaCl, 3 KCl, 2 MgCl2, 2 CaCl2, 1.25 NaHPO4, 26.5 NaHCO3, and 20 D-glucose. Picrotoxin and Nefidipine (Tocris Bioscience) were used at 10 μM in ACSF.

Calcium imaging and analysis – Widefield Tbr1KO experiments. Cultured brain slices were removed from the incubator and held in oxygenated ACSF at 28°C for 1–2 h. Slices were then immersed in oxygenated ACSF containing the $[Ca2^{+}]$i-indicating dye Fluo-4 (30 μM) and 0.07% Pluronic F-127 (Invitrogen) for 45–50 min, rinsed, and placed into a glass-bottomed experimental chamber under an Olympus AZ100 or Olympus MDX microscope with high speed CCD Cameras attached. Oxygenated ACSF (31°C-33°C) was superfused into the acquisition chamber continuously during experiments, and the slice was allowed to rest for thirty minutes under these conditions before experiments began. Whole slice, low magnification fluorescence images were captured at 1 Hz.

Calcium imaging and analysis for single cell resolution experiments – Brain slices were prepared as for widefield imaging experiments, but placed into a glass bottom chamber mounted above an Olympus spinning disk confocal microscope. To date, most studies of calcium transients in identified cell populations have utilized dissociated cultures. We developed a unique system for measuring calcium signals in genetically labeled cell populations in an intact brain slice preparation. Images are acquired with 20x or 40x objective magnification. To begin an acquisition, first a single confocal image of interneuron morphology (RFP) was acquired with the DSU spinning disc unit, which is necessary to resolve cellular structures amidst bright labeling from the tdtomato labeling system. Next confocality was turned off and a timelapse was collected with GFP filters of widefield fluo4 fluorescence. Widefield imaging enables faster acquisition speeds with lower dye bleaching than what would be achieved with confocality, which is important when working with calcium indicator dyes that will be used in long experiments including drug application. Additionally the use of an inverted microscope flattens the surface of the slice such that we are able to obtain an even plane of focus even across an entire field of view acquired with 20x objective magnification. The high dynamic range of this dye leads to a very strong signal to noise ratio, such that in widefield images, individual cells in the GFP channel are seen more clearly than in confocal images from RFP labeled cells in the

same field of view. Our system is able to clearly resolve cellular structures and identify genetically labeled interneurons using the DSU in the RFP channel, with the use of widefield fluo4 imaging allowing a signal to noise ratio in calcium imaging experiments that is on par with that from more expensive confocal systems, but with much better resistance to dye bleaching.

Tiled image acquisition and Analysis – Tiled images were acquired on the Olympus DSU system previously described. Slices were cut as if for culture, but then immediately placed into the imaging chamber rather into culture media. Imaging area was set to include a majority of the neocortex on one hemisphere of a slice, and automated software used either the 20x or the 40x objective to image the entire field of view and stitch smaller images into a large one of the entire area imaged. Interneuron distribution was quantified across cortical layers by counting interneurons in 10 evenly spaced bins set up spanning the depth of the cortex. Bin 1 one was positioned just below the pial surface, and bin 10 located just above the subventricular zone. The width of each bin was held constant between slices, but the length was changed to fit the size of the cortex. Total number of cell in each bin was was divided by the area of the bin to convert cell counts to density measurements.

Results

Waves occur in Tbr1 KO cortex in appropriate locations at normal relative frequencies

In previous experiments we described the development of waves of activity in the cortex. (Conhaim et. al. 2011) We showed that, at early stages of wave occurrence, activity occurs at high frequencies in the piriform cortex and a subset of those waves are able to propagate past the rhinal fissure and into the neocortex. The frequency of waves in the piriform cortex peaked between P1 and P3 at around 3.5-4 events per minute, while the frequency of events in the neocortex at these stages was between 0.5 and 0.8 events per minute. At later stages, P6-P7, wave frequencies were lower. In the current set of experiments we measure wave frequencies in the piriform and neocortex at two developmental time points in the Tbr1 KO to determine whether the same developmental profile of wave activity exists in the absence of Tbr1.

Upon quantification of wave activity recorded in Tbr1 KO slices, we found that at early stages, the frequency of activity in the piriform cortex was significantly greater than that of the neocortex, just as was observed in Conhaim et. al. 2011. The respective wave frequencies in piriform and neocortex were 4.33 ± 1.06 (SEM) and 0.61 ± 0.13 events per minute ($p=0.007$). At later stages, as in previous experiments in wild type animals, piriform activity was greatly reduced to 1.50 ± 0.26 events per minute, while neocortical activity had increased slightly to 1.13 ± 0.27 events per minute such that the difference in the rate of wave occurrence in piriform vs neocortex was no longer significant ($p=0.16$). This likely reflects an increase the fraction of waves which propagate out of the piriform cortex into the neocortex as the overall frequency of waves in the piriform cortex declines.

GABA contributions to Tbr1 KO waves are normal

Although the relative frequencies of waves in the two regions of cortex were normal, we reasoned that this might have occurred through compensatory mechanisms activated by the distressed cortical network. As the two neurotransmitters involved in generating cortical waves are GABA and glutamate (Conhaim et. al. 2011, Easton et. al. 2014), we investigated the role of GABA in generating waves in the Tbr1 KO under the hypothesis that an increase in excitatory GABA signaling compensates for a lack of glutamatergic drive from the Tbr1 deficient pyramidal neurons. In previous experiments we showed that the high frequency activity observed in the piriform cortex was supported by excitatory GABA, whereas the lower frequency activity which is more likely to propagate into the neocortex was more dependent on glutamatergic neurotransmission.

However in the current experiments, the sensitivity of wave activity to GABA blockade at early and late stages in the Tbr1 KO followed

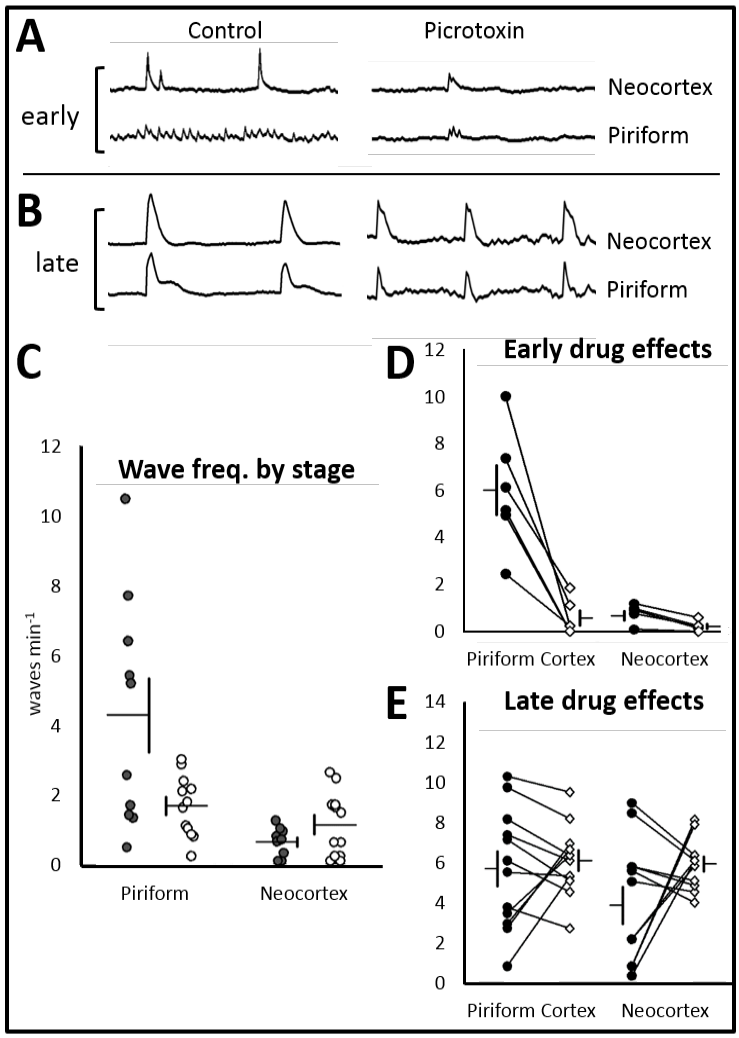

Figure 1: Waves of activity persist in slices of Tbr1KO cortex and retain sensitivity to GABA blockade. Parts **A** vs **B** depict calcium fluorescence records in early versus late stages of cortical wave expression. Early includes P2-P3 (E17 + 2-3DIV) slices while late includes P6-P7(E17 + 2-3DIV) slices. The frequency of calcium transients such as those depicted in **A,B** are shown in scatterplot **C**. High frequencies of small amplitude calcium transients are observed in early piriform cortex but not in later piriform cortex. The frequency of activity in the neocortex increases. Part **D** shows the effect of picrotoxin on early stage activity, while part **E** shows the effect of picrotoxin on late stage activity. Picrotoxin is more likely to increase activity at later stages.

previously reported trends. In early slices the frequency of waves in both piriform and neocortex was significantly reduced by picrotoxin application. The frequency of waves in piriform cortex decreased 91% from 6.40 ± 1.11 to 0.60 ± 0.80 events per minute (p=0.003). In the neocortex event frequencies dropped 70% from 0.69 ± 0.20 to 0.21 ± 0.23 events per minute (p=0.015). At later stages, activity was seen to increase frequency upon application of picrotoxin, although observed changes in frequency were not statistically significant. Wave frequencies in the piriform cortex increased 7.4% from 1.67 ± 0.26 to 1.79 ± 0.15 events per minute (p=0.59). In the neocortex, a larger change was observed, with event frequencies increasing 55% upon picrotoxin application from 1.13 ± 0.27 to 1.74 ± 0.11 events per minute (p=0.092). In six cases where the glutamate AMPA receptor blocker CNQX was applied, wave activity was completely abolished in all regions.

The distribution of interneurons in Tbr1KO cortex mimics that seen in reeler knockout mice

The in-tact GABA contribution to wave activity in the Tbr1 KO was surprising, as this indicates that the GABAergic network is able to innervate the neocortex despite disturbances to normal cortical architecture that might be expected to remove necessary cues for GABAergic network development. Few studies to date have investigated the effects of Tbr1KO, which selectively affects differentiation of cortical excitatory neurons, on the innervating network of inhibitory GABAergic interneurons that regulates the activity of these excitatory cells. We used confocal imaging of RFP and GFP labeled inhibitory interneurons to analyze the

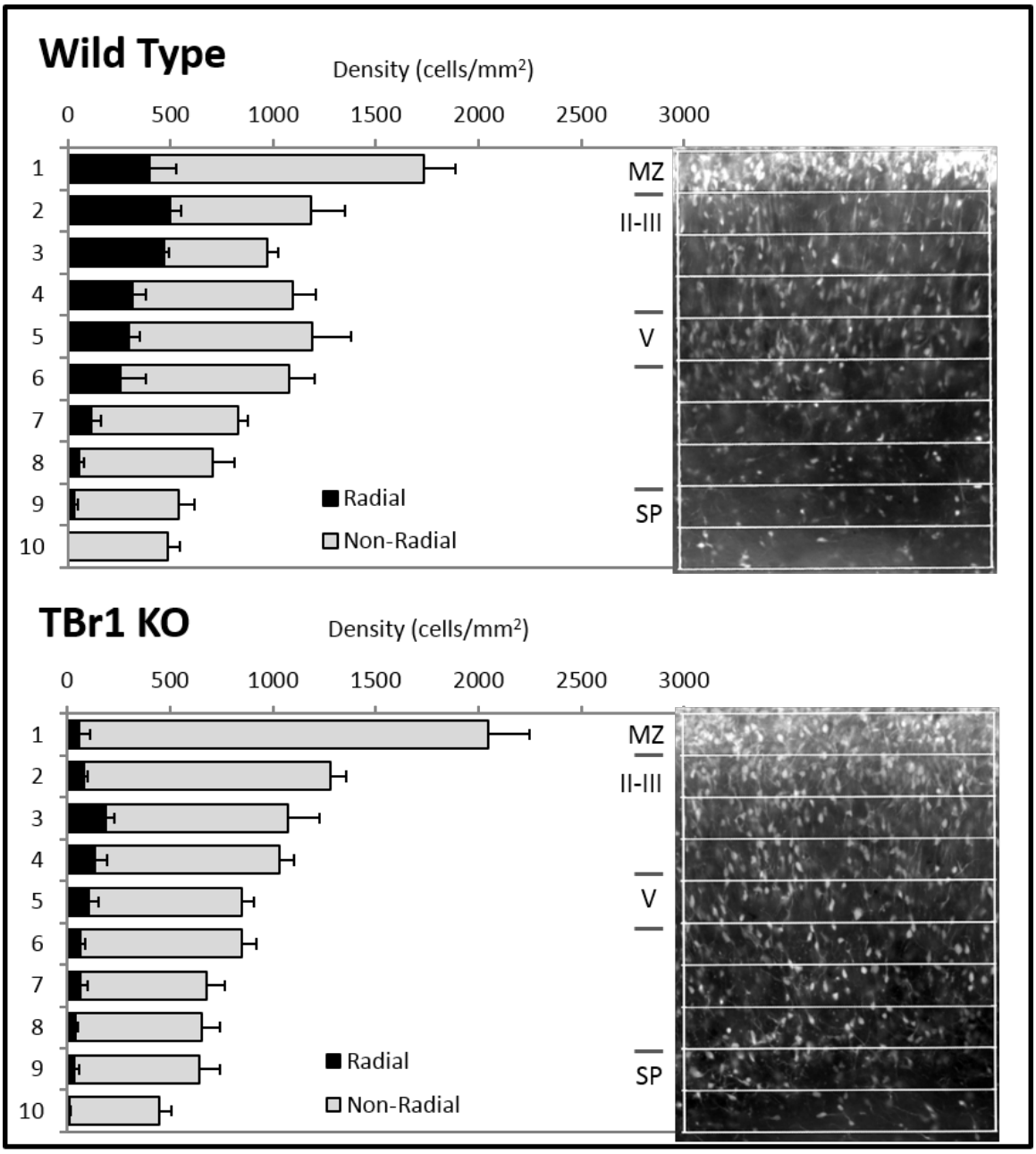

Figure 2: Tbr1 KO disrupts the layer positioning of XFP labeled interneurons. The density of genetically labeled interneurons is plotted in 10 bins spanning the pial surface to the edge of the cortical subventricular zone for control and Tbr1 KO conditions. In the wild type condition bins 1-3 approximate the still developing layers II-III which are marked by a high density of interneurons with a marked bipolar morphology. Bin 5 in controls depicts a high density of total labeled interneurons consistent with the normal high density of interneurons in cortical layer 5. In the Tbr1KO condition, a reduction in layer 5 cells is observed. Additionally, radially oriented cells are reduced in number in superficial layers of the Tbr1 KO

distribution and morphology of interneurons in the Tbr1KO cortex. Tiled images, using 20 and 40x objective magnifications, were collected that spanned the entire depth of the neocortex. Interneuron distribution was quantified across cortical layers by counting interneurons in 10 evenly spaced bins set up spanning the depth of the cortex. Bin 1 one was positioned just below the pial surface, and bin 10 located just above the subventricular zone. The total number of cells in each bin was quantified. Additionally, a subset of interneurons were identified as "radially oriented". These cells were identified by having just two bipolar processes oriented perpendicular

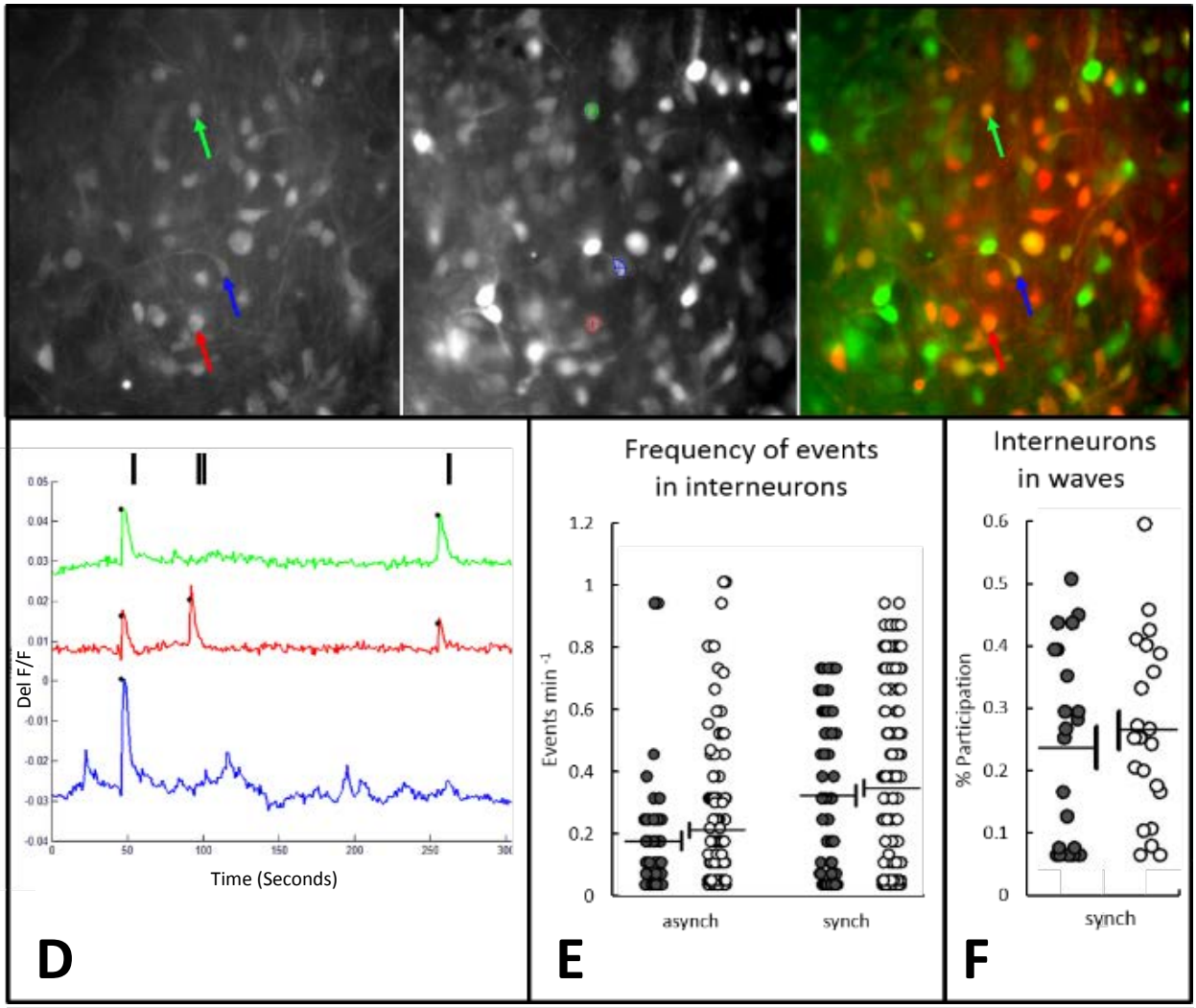

*Figure 3: RFP labeled interneurons have two types of calcium transient*s. **A** depicts RFP labeled interneurons viewed with confocal microscopy. **B** depicts same cells with widefield imaging of fluorescent calcium indicator dye fluo4. **C** shows RGB merge of these images with dual-labeled cells in yellow. Regions of interest are drawn on the RFP image over cells marked with arrows in **A**. In **B** those regions are shown over the same cells in the calcium record from the same slice. **D** shows mean fluorescence intensity over time from the three regions indicated in **B**, each corresponding to one cell. Synchronous wave activity is marked with one bar, asynchronous activity is marked with two bars. **E** shows that the frequency of both asynchronous and synchronous activity is unchanged in control (dark circles) versus Tbr1 KO (light circles) conditions. In **E**, percent of interneuron participation is quantified for twenty waves each from control and Tbr1 KO conditions. Average % interneurons participating in individual waves is unchanged in control versus Tbr1 conditions.

to the pial surface, potentially with the cell soma distended in the same direction. These cells were also counted and quantified in each of the 10 bins for every slice.

The data in Figure 2 represents the average density of cells counted in each bin across 6 control and 6 Tbr1 KO slices. The only bin that showed a significant difference in the total density of cells observed in control vs KO conditions was bin 5, corresponding to cortical layer 5 which normally has a high density of interneurons. The region had an average density of 1384.81 ± 48. cells/mm^2 in control conditions and 848.33 ± 48.7575 cells/mm^2 in the KO (p= 0.024). Bins 1-4 all showed significant decreases in the number of radially oriented cells observed in each bin in control vs KO conditions. Bin1 had densities of 466.74 ± 130.65 and 59.03 ± 49.53 cells/mm^2 (p=0.024), control and KO respectively, whereas the same values for bins 2-4 were as follows: Bin 2; 578.81 ± 58.01 and 81.65 ± 20.29 cells/mm^2 (p<0.001), Bin 3; 543.68 ± 24.86 and 190.03 ± 41.65 cells/mm^2 (p<0.001), Bin 4; 369.99 ± 64.70 and 134.95 ± 56.33 cells/mm^2 (p=0.021).

Interneurons in WT and Tbr1KO cortex participate asynchronous and synchronous calcium signals

As it has previously been proposed that waves play a role in the determination of layer location in interneuron development (de Lima et. al. 2009), we hypothesized that interneurons participate in waves. While the pharmacological data indicates that interneurons are playing a role in wave generation, this does not necessarily mean that calcium transients of interneurons are synched with those of excitatory neurons, as GABA could also be acting through tonic, non-synaptic means. We identified two types of activity in Tbr1 KO and control cells using calcium imaging of red labeled neurons: events occurring at frequencies similar to wave events that were synchronous across many cells in the field of view, and asynchronous calcium signals restricted to single cells. We found that the frequencies of each of these types of activity were unchanged in control versus Tbr1 KO conditions, with rates of 0.20 ± 0.03 events per minute and 0.23 ± 0.02 events per minute respectively for asynchronous activity (p=0.32), and 0.34 ± 0.03 events per minute and 0.36 ± 0.02 events per minute for wave activity (p= 0.56). Additionally, we analyzed each of the synchronous wave events recorded in the Tbr1KO and WT conditions and counted the fraction of interneurons participating in each wave. The percent participation of interneurons in waves was 23.71 ± 0.03 % for control and 26.55 ± 0.03 % for Tbr1 KO conditions (p=0.53) indicating that interneurons participated equally in waves in knockout and control conditions.

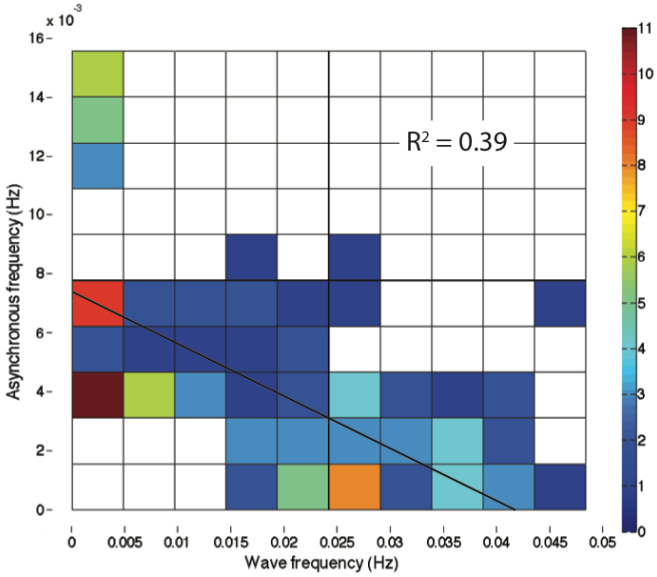

Figure 4: Asynchronous and synchronous calcium signals are negatively correlated. All cells imaged in control conditions are plotted by frequency of synchronous wave activity (x axis) and asynchronous activity (y axis). When multiple cells have overlapping frequencies they are plotted together in one box with the color of the box depicting the number of cells. See color bar on right: red depicts 11 cells and blue depicts 1 cell.

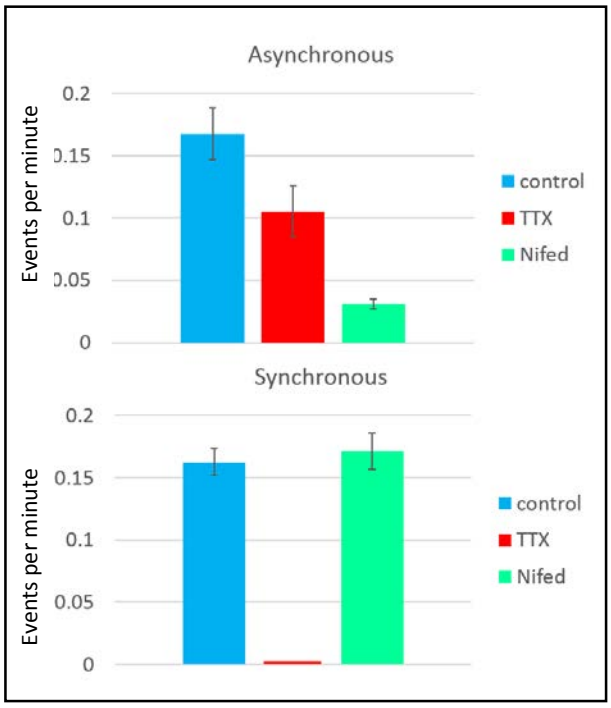

Figure 5: Asynchronous activity is dependent on L-type calcium channels while synchronous activity requires sodium channels. The frequency of events is plotted for asynchronous activity (top) and synchronous activity (bottom). Control frequencies are shown in blue, frequencies with the sodium channel blocker TTX applied shown in red, and activity frequencies with L-type calcium channel blocker nifedipine shown in green.

Asynchronous activity is sensitive to blockade of L-type calcium channels whereas synchronous activity is sensitive to blockade of sodium channels

We next hypothesized that cells participating in asynchronous calcium signaling would be less likely to participate in synchronous activity, and vice versa. We plotted each cell with its participation in synchronous activity on the X axis and participation in asynchronous activity on the y axis (Figure 4). After fitting a linear regression to this data, we found an R^2 value of 0.39. A significance test of this data gave $p<0.001$, indicating the negative correlation was significant. We followed this study by examining the sensitivity of the two types of blockers to pharmacological blockade. Given previous groups describing L-type calcium channel mediated calcium transients in immature migrating cells (Bortone et. al. 2009) and the dependence of synchronous wave activity on sodium-dependent action potential firing, we constructed the following hypotheses: Blockade of L-type calcium channels with nifedipine will leave synchronous activity intact while abolishing asynchronous activity, while blockade of sodium channels with TTX will abolish synchronous activity while leaving asynchronous activity intact. Figure 5 shows this hypothesis to be correct. In control conditions the frequency of asynchronous wave activity was 0.168 ± 0.021 (SEM) events per minute, and this was reduced only 37.2% to 0.106 ± 0.021 events per minute in unpaired experimental slices exposed to TTX ($p=0.039$, unpaired student ttest). In experimental conditions where nifedipine was applied instead of TTX, asynchronous activity was reduced 81.4% to 0.031 ± 0.004 events per minute ($p<0.001$, unpaired student ttest). Synchronous wave activity had similar control frequencies but responded much differently to the same pharmacological blockers. Control slices exhibited average synchronous activity frequencies of 0.162 ± 0.011 events per minute, and this increased slightly, 5.4% to 0.146 events per minute in unpaired experimental slices exposed to nifedipine, though the increase was not significant ($p=0.63$, unpaired student ttest). Synchronous activity was completely abolished in all slices exposed to TTX ($p<0.001$, unpaired student ttest).

Conclusions

These results indicate that mice expressing Tbr1 KO have calcium waves in the cortex at normal frequencies and with normal neurotransmitter dependencies. This result highlights the ability of cortical waves to persist in spite of numerous changes to the cortex

associated with Tbr1 KO, including aberrant intra and extra cortical connections, disorganized cortical layers (Hevner et. al. 2001), and a reduced and disorganized subplate (Hevner et. al. 2002). Previous studies have indicated that each of these factors could be expected to prevent waves of activity. For example, a critical role of the subplate has been proposed in propagating wave activity out of ventral progenitor regions and into the neocortex due to the extensive connectivity of the subplate and relative maturity of cells located there (Luhmann et. al. 2003, Hanganu et. al. 2009, Lischalk et. al. 2009). Additionally, intact connections between the cortex and other regions such as the thalamus have been proposed necessary for spontaneous activity patterns (Yang et. al. 2009), and Namiki et. al. 2013 stated that layer III neurons initiated cortical waves and proposed a critical role for these cells in wave generation. If layer III neurons or subplate cells are indeed critical for wave generation, and it is their unique connectivity that allows propagation of activity out of these cells, then wave activity should be blocked in the Tbr1KO. Our results do not rule out a role for layer III or subplate neurons in generating cortical waves, as the disorganized cortex would still contain these cells in abnormal locations, albeit potentially in smaller numbers (Hevner et. al. 2001). However, our results do indicate that the normal positioning and connectivity of these cells is not necessary for wave generation. Thus any ability of layer III or subplate neurons to generate waves is more likely to be a result of preserved intrinsic ion channel properties in these cells, and the propagation of depolarization generated by these channels to other cells could be carried through the extracellular space or short range connections present in the Tbr1KO. Robust compensatory mechanisms for maintaining wave activity in the presence of pharmacological blockers have been reported, for example in the spinal cord (Chub and O'Donovan 1998). But the current experiments are a unique example showcasing the ability of wave activity to overcome gross changes to the cortical organization.

However, preserved ion channel properties of cells is not necessarily the reason for continued wave generation in the Tbr1KO. It is also possible that wide scale compensatory mechanisms are at play allowing waves to continue despite reduced drive from the glutamatergic neural network. The latter proposition holds merit, given unpublished microarray data from the Hevner lab indicating that in P0 Tbr1 KO cortex there are significant reductions in a wide variety of voltage gated sodium and calcium channels, metabotropic and ionotropic glutamate receptors, and GABA receptor subunits, all of which play roles in wave generation and regulation. Given that wave activity in the neocortex is normally permitted by relatively weak GABAergic inhibition, we sought to examine whether an increase in excitatory GABA neurotransmission (which drives wave activity in the piriform cortex) might be responsible for wave generation in the Tbr1 KO neocortex. To answer this we exposed slices of Tbr1 KO mouse brain expressing wave activity to picrotoxin, a $GABA_A$ receptor blocker. Previous experiments from the Moody lab have shown that high frequency activity at early stages, restricted to ventral cortex, is sensitive primarily to blockade of GABAergic neurotransmission, whereas fully propagating activity at later stages is primarily sensitive to glutamatergic blockade and GABA blockade may even induce activity Conhaim et. al. 2011). This is likely reflective of a two-pacemaker system (Easton et. al. 2014) wherein early waves are generated by a GABAergic pacemaker region which is very active early in wave expression, while later in development the GABA pacemaker fades out while a glutamatergic pacemaker, responsible for fully propagating waves, becomes dominant. The same trends were found here in the Tbr1 KO mouse, with high frequency ventral activity showing a greater ability to be blocked by picrotoxin than later activity in the neocortex. This

indicates that remaining wave activity in the Tbr1KO is not occurring due to a shift towards GABA excitation or expression of the GABAergic pacemaker outside of its normal range of operation.

Parallel with drug experiments examining GABA contributions to waves, we examined the morphology of the interneuronal network using RFP and GFP labeling of interneurons in WT and Tbr1 deficient mice to ensure that the cortex was receiving GABAergic innervation. To date, few studies have examined the morphology of GABAergic interneurons in the Tbr1KO. The closest related study is Hevner et. 2006, which studied the reeler mutation. Reeler mice lack reelin, which is a signaling molecule downstream of Tbr1 critical for the placement of cortical excitatory neurons into appropriate layers. Reelin is expressed in cajal retzius cells at the pial surface of the developing cortex, and attracts newborn neurons in the ventricular zone towards the pial surface to establish the "inside out" cortical structure. Likely the disorganization of cortical layers in Tbr1KO is due to down-regulation of reelin with Tbr1 KO. Our experiments provided an additional level of detail over previous experiments: the use of an XFP reporter for interneurons allowed classification of labeled cells into groups based on cell morphology due to the membrane localization of XFP and consequent labeling of cellular processes. We identified cells that had a bipolar, radial orientation. We found that such cells in the Tbr1 KO were of lower number and distributed throughout the cortex rather than concentrated at the pial surface, as in control animals. This result provides further evidence of a breakdown of the "inside out" cortical structure in the Tbr1 KO, as the immature migrating interneurons are no longer concentrated under the pial surface of the developing cortex. It is likely that many of the neurons not identified as "radially oriented" are also immature migrating neurons, but the decreased ability to identify interneurons aligned in the direction of radial glial fibers is a good indicator of disorganization in Tbr1 KO cortex. In counting total density of interneurons across cortical layers, we found a decrease particularly in the density of layer 5 neurons in the Tbr1KO. In fact the distribution of interneurons in the Tbr1KO mimicked that seen by Hevner et. al. 2004, where the distribution of immunolabeled interneurons in reeler mice also lacked the higher density of interneurons in layer 5. Hevner et. al. 2004 thoroughly described the time of origin of cells located at various cortical depths in control and reeler mice, and determined that despite the disorganization of the cortex in the reeler knockout, excitatory and inhibitory neurons born on the same day of development still managed to find each other in the same cortical layers of the reeler mouse.

The persistence of waves in the Tbr1 KO is interesting in light of the conclusions of Hevner et. al. 2004. The level to which interneuron distribution in the Tbr1 KO resembled that of the reeler mouse indicates that the layer inversion in the Tbr1 KO may be due to the downregulation of reelin as Tbr1 is upstream of reelin. Hevner et. al. 2002 stated that, even in the reeler KO, some level of layer organization remained, as inhibitory neurons were still able to find a layer location that included excitatory neurons of the same age as the inhibitory neurons. They proposed that this occurred due to some signal from the excitatory neurons to the inhibitory neurons. Given evidence from other labs that waves play a role in terminating interneuron migration, (Voigt et. al. 2009) we decided to test whether wave activity could be that signal. We examined whether interneurons were participating in waves in the Tbr1 KO, which recapitulate the interneuron disorganization observed in reeler mice. We found that interneurons indeed participated in waves, and the percentage of interneurons participating in each wave was no different from that observed in control conditions.

Finally, in imaging calcium activity in RFP labeled interneurons, we identified two distinct

forms of activity in these immature cells: a synchronous signal (waves), and an asynchronous signal restricted to individual cells. We found that the synchronous signal was selectively sensitive to blockade of sodium channels, whereas the asynchronous signal was sensitive to blockade of L-Type calcium channels. Although other experiments have identified calcium signals in individual interneurons (Bortone et. al. 2009, de Lima et. al. 2009), these experiments allowed imaging of interneurons in a complete brain slice preparation with an extremely high signal to noise ratio made possible by the utilization of RFP labeled interneurons and green calcium indicator dyes. The significance of the two forms of activity must be examined in further studies, but Bortone et. al. 2009 proposed that nifedipine sensitive calcium signals in development provide a pro-migratory signal that is turned off by upregulation of the KCC2 transporter and the onset of GABA inhibition. De Lima et. al. 2009 showed that participation in synchronous calcium signals in dissociated cultures terminated cell migration, and McCabe et al. 2009 showed that blocking wave activity during a critical window delayed the onset of GABA inhibition. Thus the current experiments could indicate sequentially expressed forms of activity with distinct effects on cell migration, with asynchronous single cell activity encouraging migration until participation of the cell in wave activity upregulates KCC2 and provides a stop signal for migration and helps the cell find appropriate cortical layer depth.

References

Blankenship AG, Feller MB (2010) Mechanisms underlying spontaneous patterned activity in developing neural circuits. Nat Rev Neurosci. 11:18-29.

Bortone D, Polleux F (2009) KCC2 expression promotes the termination of cortical interneuron migration in a voltage-sensitive calcium-dependent manner. Neuron. 62(1):53-71.

Chub N, O'Donovan MJ (1998) Blockade and recovery of spontaneous rhythmic activity after application of neurotransmitter antagonists to spinal networks of the chick embryo. J Neurosci. 18:294-306.

de Lima AD, Gieseler A, Voigt T (2009) Relationship between GABAergic interneurons migration and early neocortical network activity. Dev Neurobiol. 69(2-3):105-23.

Garaschuk O, Linn J, Eilers J, Konnerth A. (2000) Large-scale oscillatory calcium waves in the immature cortex. Nature Neurosci. 3: 452-459.

Hevner RF, Daza RA, Englund C, Kohtz J, Fink A (2004) Postnatal shifts of interneuron position in the neocortex of normal and reeler mice: evidence for inward radial migration. Neuroscience 124(3):605-18.

Hevner RF, Miyashita-Lin E, Rubenstein JL (2002) Cortical and thalamic axon pathfinding defects in Tbr1, Gbx2, and Pax6 mutant mice: evidence that cortical and thalamic axons interact and guide each other. J Comp Neurol. 447(1):8-17.

Hevner RF, Shi L, Justice N, Hsueh Y, Sheng M, Smiga S, Bulfone A, Goffinet AM, Campagnoni AT, Rubenstein JL (2001) Tbr1 regulates differentiation of the preplate and layer 6. Neuron. 29(2):353-66.

Khazipov R, Luhmann HJ. 2006 Early patterns of electrical activity in the developing cerebral cortex of humans and rodents. Trends Neurosci. 29(7):414-8.

Kilb W, Kirischuk S, Luhmann HJ. (2011) Electrical activity patterns and the functional maturation of the neocortex. Eur J Neurosci. 34(10):1677-86.

Lischalk JW, Easton CR, Moody WJ. (2009) Bilaterally propagating waves of spontaneous activity arising from discrete pacemakers in the neonatal mouse cerebral cortex. Dev. Neurobiol. 69:407-14.

McCabe AK, Easton CR, Lischalk J, Moody, WJ (2007) Roles of glutamate and GABA receptors in setting the developmental timing of spontaneous synchronized activity in the developing mouse cortex. Dev. Neurobiol. 67:1574-1588.

Moody WJ and Bosma MM (2005) Ion Channel Development, Spontaneous Activity, and Activity-dependent Development in Nerve and Muscle Cells. Physiol. Rev. 85:883-941.

Namiki S, Norimoto H, Kobayashi C, Nakatani K, Matsuki N, Ikegaya Y. 2013 Layer III neurons control synchronized waves in the immature cerebral cortex. J Neurosci. 33(3):987-1001.

Scott A, Weir K, Easton C, Huynh W, Moody WJ, Folch A (2013) A microfluidic microelectrode array for simultaneous electrophysiology, chemical stimulation, and imaging of brain slices. Lab Chip 13:527-535.

Tamamaki N, Yanagawa Y, Tomioka R, Miyazaki J, Obata K, Kaneko T (2003) Green fluorescent protein expression and colocalization with calretinin, parvalbumin, and somatostatin in the GAD67-GFP knock-in mouse. J Comp Neurol. 467:60-79.

Wong WT, Myhr KL, Miller ED, Wong RO (2000) Developmental changes in the neurotransmitter regulation of correlated spontaneous retinal activity. J Neurosci. 20:351-60.

Yang JW, Hanganu-Opatz IL, Sun JJ, Luhmann HJ (2009) Three patterns of oscillatory activity differentially synchronize developing neocortical networks in vivo. J Neurosci 29: 9011-9025.

Yang JW, An S, Sun JJ, Reyes-Puerta V, Kindler J, Berger T, Kilb W, Luhmann HJ (2013) Thalamic network oscillations synchronize ontogenetic columns in the newborn rat barrel cortex. Cereb Cortex 23: 1299-1316.

General Conclusions

The many roles of GABA in wave activity of the developing cortex

In the previous chapters we tested several hypotheses about the role of GABAergic neurotransmission in developing neocortex. First we showed that the changing appearance of waves of neocortical activity was due to a shift in neurotransmitter dependency of waves from GABAergic early in development to glutamatergic later on. Next, we used mice with a mutation in GAD1, the gene responsible for the majority of GABA synthesis, to test the hypothesis that the changing neurotransmitter dependencies of wave activity was due to the emergence of a second pacemaker for wave activity. We showed that there are two neural networks in the ventral cortex capable of generating wave activity: one GABAergic that triggers waves restricted to ventral cortex, and a second glutamatergic pacemaker that is able to propagate waves into the dorsally located neocortex. Simultaneously with its function in generating wave activity in the ventral cortex, GABA plays a role in dampening network oscillations observed in dorsal neocortex.

BROADER IMPACTS: These findings have implications for the identification and treatment of disease in the nervous system. Studies using EEG recordings have been used to examine cortical activity in third trimester, premature infants (Milh et. al. 2007), and the activity observed in these studies appears similar to the population activity observed in the cortex during first postnatal week of mice. Understanding the normal patterns of population activity could be useful in predicting future problems with premature infants. Additionally, understanding the roles of GABA first in generating wave activity and ultimately terminating waves due to the appearance of GABA inhibition may provide insight into a group of related conditions identified wherein patients experience imbalances in the ratio of excitatory versus inhibitory neurotransmission in particular brain regions. These conditions include epilepsy and autism (Rubenstein et. al. 2003 Review). Epilepsy is characterized by unregulated electrical discharges simultaneously in large neural populations, and such dysregulation could be caused either by excessive neural stimulation via such neurotransmitters as glutamate, or insufficient regulation by the inhibitory interneurons of the brain. Autism may be caused by dysregulation in areas of the brain important for normal social interactions. Thus the findings presented in this thesis work are significant when considered in the context of these diseases. If epileptiform activity is found to resemble that observed in development, it could be that some forms of epilepsy actually represent normal developmental activity patterns expressed beyond their normal windows of occurrence. The complex nature of GABA observed in the second chapter of this study further elucidates the roles GABA plays in stimulating versus inhibiting particular cell populations, and this knowledge will help us to understand the way GABA interacts with neural networks in a variety of situations including those of the epileptic or autistic mind.

Wave activity in Tbr1 mutant mice and a putative role for waves in determining cortical layer positioning of inhibitory interneurons

In the final set of experiments we examined wave activity in transgenic mice missing the transcription factor Tbr1, hypothesizing that the structural abnormalities observed in the absence of Tbr1 would disallow wave activity. We found this not to be the case, as waves appeared at normal frequencies and with normal neurotransmitter dependencies. Interestingly, whereas the GAD67 knockout (KO) mouse showed no changes in interneuron morphology or distribution, interneurons of the Tbr1 KO mouse were highly disturbed. They were disturbed in a manner similar to that observed in reeler mice

(Hevner et. al. 2004), which express a mutation where excitatory neurons are improperly placed in the developing cortex due to lack of the signaling molecule reelin. As Hevner et. al. 2004 discussed the possibility that interneurons followed a cue from excitatory neurons to determine layer positioning in both wildtype animals and the reeler mutant, we found the possibility that wave activity might aid layer positioning of interneurons to be highly intriguing and derived a set of experiments to begin addressing this hypothesis.

If wave activity really affects the layer positioning of inhibitory interneurons, then one should observe distinct forms of activity in these cells, representing differing states of maturity in cells undergoing distinct developmental programs. By genetically labeling interneurons with red fluorescent protein and examining calcium signaling in these cells, we were able to observe to distinct forms of activity that were negatively correlated in individual cells. One: an asynchronous calcium signal, restricted to single cells, which is sensitive to blockade of L-type calcium channels. And two: a synchronous calcium signal, correlated across many cells in the field of view, which is sensitive to blockade of voltage gated sodium channels.

BROADER IMPACTS: This set of experiments is interesting first for its contrast to the results of experiments studying the GAD67 gene mutation. Whereas wave activity was grossly affected in the GAD67 KO animal, the morphology of cortical interneurons was mostly unaffected. By contrast, wave activity in the Tbr1 KO was mostly in-tact while the morphology of interneurons was highly disturbed. At first glance it would appear that the signaling-molecule-mediated changes to brain structure have a greater effect than activity-dependent changes. However, this may not actually be the case, as some organization remaining in the Tbr1 KO or reeler mice may actually have been due to electrical signaling allowing excitatory and inhibitory neurons to connect to each other in an organized fashion, despite being located in abnormal layers.

Previous groups have identified potential roles for electrical activity in the development of interneurons that are consistent with the types of activity observed in this study. (de Lima et. al. 2009, Bortone et. al. 2009) And while the developmental processes regulated by activity-dependent-signaling may be less pronounced than those observed in the Tbr1 KO, many disease conditions, such as epilepsy or autism, are likely to involve relatively minor changes to brain structure. Patients may be highly functioning despite having autistic or epileptic tendencies. Minor changes to interneuron distribution incurred due to problems with participation of immature interneurons in population activity could upset the excitatory/inhibitory signaling balance of the mature brain. Additionally, researchers are beginning to use implantation of interneurons in rodent studies to treat epilepsy (Hunt et. al. 2013), and understanding the necessary activity profiles that must be expressed by developing interneurons may help teach us how to stimulate implanted cells to maximize viability. For example, implanted cells could be genetically programmed to express ion channels inducing just the right amount of electrical activity to stimulate their migration and integration into cortical circuits. Thus the basic methods of identifying inhibitory interneurons and their calcium signals have far reaching impact on understanding and treating neurological disease.

References

Asada H, Kawamura Y, Maruyama K, Kume H, Ding RG, Kanbara N, Kuzume H, Sanbo M, Yagi T, Obata K (1997) Cleft palate and decreased brain gamma-aminobutyric acid in mice lacking the 67-kDa isoform of glutamic acid decarboxylase. Proc Natl Acad Sci USA 94:6496–6499.

Bortone D, Polleux F (2009) KCC2 expression promotes the termination of cortical interneuron migration in a voltage-sensitive calcium-dependent manner. Neuron. 62(1):53-71.

de Lima AD, Gieseler A, Voigt T (2009) Relationship between GABAergic interneurons migration and early neocortical network activity. Dev Neurobiol. 69(2-3):105-23.

Hevner RF, Daza RA, Englund C, Kohtz J, Fink A (2004) Postnatal shifts of interneuron position in the neocortex of normal and reeler mice: evidence for inward radial migration. Neuroscience 124(3):605-18.

Hunt RF, Girskis KM, Rubenstein JL, Alvarez-Buylla A, Baraban SC. (2013) GABA progenitors grafted into the adult epileptic brain control seizures and abnormal behavior. Nat Neurosci. Jun;16(6):692-7.

Milh M, Kaminska A, Huon C, Lapillonne A, Ben-Ari Y, Khazipov R. (2007) Rapid cortical oscillations and early motor activity in premature human neonate. Cereb Cortex. Jul;17(7):1582-94.

Rubenstein JL, Merzenich MM. (2003) Model of autism: increased ratio of excitation/inhibition in key neural systems. Genes Brain Behav. Oct;2(5):255-67. Review.